Technical Notes on Volume Averaging in Porous Media I: How to Choose a Spatial Averaging Operator for Periodic and Quasiperiodic Structures.

Yohan Davit, Michel Quintard

Technical Notes on Volume Averaging in Porous Media I: How to Choose a Spatial Averaging Operator for Periodic and Quasiperiodic Structures

Yohan Davit[1] · **Michel Quintard**[1]

Abstract This paper is a first of a series aiming at revisiting technical aspects of the volume averaging theory. Here, we discuss the choice of the spatial averaging operator for periodic and quasiperiodic structures. We show that spatial averaging must be defined in terms of a convolution and analyze the properties of a variety of kernels, with a particular focus on the smoothness of average fields, the ability to attenuate geometrical fluctuations, Taylor series expansions, averaging of periodic fields and resilience to perturbations of periodicity. We conclude with a set of recommendations regarding kernels to use in the volume averaging theory.

Keywords Upscaling · Volume averaging · Spatial averaging operator · Convolution · Kernel

List of symbols

Roman symbols

B	Closure dyadic for the velocity perturbation
b	Closure vector for the pressure perturbation
e	Basis vector
g	Gravitational acceleration
I	Identity dyadic
K	Permeability tensor
v	Velocity vector

✉ Yohan Davit
yohan.davit@imft.fr

[1] Institut de Mécanique des Fluides de Toulouse (IMFT), Université de Toulouse, CNRS, INPT, UPS, Toulouse, France

$\mathbf{x}$	Position vector
$\mathbf{X}_i$	Position vector for the center of unit cell i
a	A periodic scalar field
a_0	Constant part of a in the Taylor series
C	Normalization constant
i	Imaginary unit
m	Convolution kernel in the spatial averaging operator
P	Pressure
p	Width of the averaging window
$P^* =$	$P - \mathbf{x} \cdot \rho\mathbf{g}$ with $\mathbf{x} \cdot \rho\mathbf{g}$ the hydrostatic pressure
P_0	Reference pressure in the hydrostatic problem
R	One-dimensional rectangular function
T	One-dimensional triangular function

Abbreviations

VAT	Volume averaging theory

Function spaces

$C^k(\mathbb{R}^n)$	Class C^k functions in $\mathbb{R}^n$
$C_c^k(\mathbb{R}^n)$	Compactly supported class C^k functions in $\mathbb{R}^n$
$L^1(\mathbb{R}^n)$	Integrable functions in $\mathbb{R}^n$
$L^2(\mathbb{R}^n)$	Square integrable functions in $\mathbb{R}^n$

Greek symbols

$\boldsymbol{\xi}$	Position vector pointing inside the averaging volume
χ^f	Indicator function of the fluid domain
χ_0^f	Constant part of χ^f in the Taylor series
δ	Dirac delta
μ	Dynamic Viscosity
ϕ	Porosity
ρ	Density
ε	Small parameter, $\varepsilon \ll 1$

Subscripts

$\cap$	Reference symbol for the mollifier
$\cap\sim$	Reference symbol for the windowed sinc function
$\sim$	Reference symbol for the sinc function
$\sqcap$	Reference symbol for the rectangular function
$\sqcap^q$	Reference symbol for the B-spline functions
$\wedge$	Reference symbol for the triangular function
D	Reference letter for Darcy
f	Reference letter for the fluid domain

Tensor operations

$\boldsymbol{\xi}^{\otimes j} = \underbrace{\boldsymbol{\xi} \otimes \cdots \otimes \boldsymbol{\xi}}_{\text{j times}}$

$\cdot$	Tensor contraction
$(\cdot)^j$	jth order contraction
$\otimes$	Tensor product

Mathematical symbols

$\lvert\mathcal{V}^f\rvert$	Volume of the fluid domain $\int_{\mathcal{V}^f(\mathbf{x})} dV$
ℓ_p	Characteristic length for the pores
ℓ_u	Characteristic length for the unit cell
∞	Symbol for infinity
$\langle \mathrm{g} \rangle^f$	Intrinsic average of g
$\langle P \rangle_c^f$	Corrected average pressure field
$\mathbb{N}^{+*}$	Strictly positive integers
$\mathbb{N}^{+}$	Positive integers
$\mathbb{R}^n$	Real coordinate space of n dimensions
$\wp_j$	Polynomial tensor product defined as $\wp_j : \mathbf{x} \to \mathbf{x}^{\otimes j}$
$\mathcal{M}_{j,q}$	jth moment of $m_{\sqcap^q}$, defined as $\mathcal{M}_{j,q} = \int_{\mathbb{R}^n} m_{\sqcap^q}(\mathbf{x})\, \wp_j(\mathbf{x})\, d\mathbf{x}$.
$\mathcal{P}'_i$	Derivative of $\mathcal{P}_i$ defined as $\mathcal{P}'_i(x) = d_x \mathcal{P}_i = x^{i-1}$ derivative
$\mathcal{P}_i$	Polynomial defined as $\mathcal{P}_i : x \to \frac{1}{i} x^i$
$\mathcal{V}(\mathbf{x})$	Averaging volume centered at point $\mathbf{x}$
$\mathcal{V}^f(\mathbf{x})$	Fluid domain in the averaging volume centered at point $\mathbf{x}$
$\mathcal{Y}$	Unit cell characterizing the periodic geometry
$\mathcal{Y}^f$	Fluid domain within the unit cell
∇	Nabla operator
$\partial\mathcal{Y}^{fs}$	Fluid–solid interface within the unit cell
$\tilde{g}$	Perturbation of $\tilde{g} = g - \langle g \rangle^f$
$\lvert_{\mathbf{x}}$	Average field evaluated at $\mathbf{x}$
sinc:	$x \to \frac{\sin(\pi x)}{\pi x}$

1 Introduction

In this series of papers, we revisit technical aspects of the volume averaging technique (VAT), as reviewed, for instance, in Whitaker (1999). This approach has proven successful in studying many different problems in porous media sciences, from Darcy's law (Whitaker 1986) in geological formations to superfluid flow in engineering structures (Allain et al. 2010), the formulation of macroscale boundary conditions between porous and fluid media (Ochoa-Tapia and Whitaker 1995; Valdés-Parada et al. 2007) or even mass transport in communities of microorganisms (Davit et al. 2013; Wood and Whitaker 1998). The contributions of many authors over a time span of several decades have led to significant evolutions of the original approach. Some of these evolutions are significant, but the volume of the literature can make it challenging to track advances from the earliest works. In this series of papers, our goal is to clarify important technical developments of the VAT and revisit several aspects of the approach.

In this paper, the first of this series, we focus on a fundamental mathematical ingredient of the method: the integral operator used to average the microscale fields. We ask the question of how to choose such a spatial averaging operator for periodic and quasiperiodic structures? A variety of definitions have been proposed in the literature. In its simplest *standard* form, the spatial average of a field g at point $\mathbf{x} \in \mathbb{R}^n$ is defined as the integral of g within a set centered at point $\mathbf{x}$, normalized by the volume of the set (Whitaker 1999). If the medium is locally periodic, a natural definition for this set would be the parallelepiped defining the unit cell (see an example two-dimensional structure in Fig. 1). If the medium is not periodic, or if the discussion remains generic, one often simply uses a sphere centered in $\mathbf{x}$ as the averaging set. A more general definition, which is very rarely used, is based on a convolution product between a kernel function and the field g. The idea is that, by *adequately* selecting the kernel in the convolution, the averaging operator can act as a low-pass filter that yields an average field with desirable properties, the exact list of desirable properties will be detailed later on. This method is used in image processing (Buades et al. 2005), signal processing (Witkin 1984) or in fluid mechanics (e.g., turbulence modeling (Sagaut 2006) and smoothed particle hydrodynamics (Monaghan 2005)). For the VAT in porous media, the idea dates back to the seminal works of C. Marle in Marle (1965, 1967), who anticipated difficulties associated with the *standard* definition that we thoroughly present in this paper, and is also discussed in Baveye and Sposito (1984), Hassanizadeh and Gray (1979), Mls (1987), Quintard and Whitaker (1994a, b), Buckinx and Baelmans (2015a, b, 2016). With this generalized definition, we can readily recover the more standard averaging operators, for example using a rectangular function for the kernel.

The problem of *adequately* selecting the kernel of the convolution, which we will term m thereafter, is central to the volume averaging method. What do we expect from this kernel? Primarily, we want it to filter out the smallest lengthscales from the microscale field, to smooth it out. In addition, our goal in using an upscaling technique is to obtain a set of partial differential equations applying to the average fields. Therefore, we also want to construct the averaging operators so that the derivatives of average fields exist and are well behaved, up to the order required. This problem was initially pointed out in Marle (1967, 1982) on a pure mathematical basis. The potential for the standard volume average to yield non-differentiable fields was also raised in a number of papers including Veverka (1981), Mls (1987). Historically, some of the potential solutions proposed in Howes and Whitaker (1985), which consisted in changing the shape of the averaging volume or making it larger, turned out

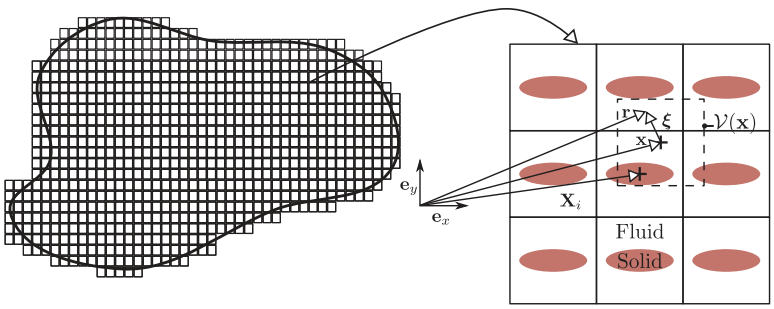

Fig. 1 Two-dimensional periodic porous medium and an example averaging volume. The unit cell i is a unit-square $[0, 1]^2$, centered at $\mathbf{X}_i$ that contains a single solid ellipse (*colored*). The *dashed unit cell*, $\mathcal{V}(\mathbf{x})$, is an example averaging set centered in $\mathbf{x}$. The standard average of g at point $\mathbf{x}$ is $\langle g \rangle^f_{\sqcap}\Big|_{\mathbf{x}} = \frac{1}{|\mathcal{V}^f|(\mathbf{x})} \int_{\mathcal{V}^f(\mathbf{x})} g(\mathbf{x}+\boldsymbol{\xi})\, d\boldsymbol{\xi}$, with $\mathcal{V}^f(\mathbf{x})$ the fluid domain (*white*) contained in $\mathcal{V}(\mathbf{x})$ and $\left|\mathcal{V}^f\right|(\mathbf{x}) = \int_{\mathcal{V}^f(\mathbf{x})} dV$

to be incorrect (Quintard and Whitaker 1994a). All these works motivated further research and proposals as discussed hereafter. A possible constraint for the kernel would be that m is sufficiently smooth, in an extreme case $C^{\infty}(\mathbb{R}^n)$, as proposed in Marle (1967, 1982), Quintard and Whitaker (1993, 1994a, b). A less extreme constraint is that only the average fields are sufficiently smooth. In fact, we use Taylor series in the VAT, so we need the average fields to be in $C^M(\mathbb{R}^n)$ with $M \in \mathbb{N}^+$ the order of the closure, i.e., the largest order of the derivatives in the approximate solution for the perturbations. Importantly, these conditions are clearly not respected for the most standard, and most used, definitions of the averaging operator for which we use a discontinuous rectangular function as a kernel. As we will see, the holes in the fields generated by the porous structure may produce discontinuities in the derivatives of the average fields, because the averaging operator does not filter out the frequencies associated with the periodic porous medium.

Besides obtaining the correct regularity conditions for the average fields, another important constraint for the choice of a kernel is the compatibility with the determination of effective properties over a single unit cell for strictly periodic media. Indeed, closure problems are solved over one unit cell with periodic boundary conditions and the closure variables are then averaged using the standard (or cellular) average to obtain the effective property. Therefore, the kernel must ensure that, when the microscale field is periodic, the average defined with the convolution is equal to the the standard average. The use of multiple averaging was proposed before to achieve these two objectives (Quintard and Whitaker 1994a, b; Buckinx and Baelmans 2016). Another class of difficulties in the definition of the averaging operator emerges from systems that are not strictly periodic, for instance when the characteristic scales of the heterogeneities vary in space. This question was investigated using the VAT for dendritic mushy zones developing during the solidification of binary mixtures (Goyeau et al. 1999) and the study of interfaces between porous media and fluid domains (d'Hueppe et al. 2011). These points are further discussed in this paper.

The remainder of this paper is organized as follows. In Sect. 2, we provide simple examples for which we observe such discontinuities and limitations of the standard definitions of the averaging operator. In Sect. 3, we go on to discuss the generalized form of the spatial averaging operator, which is defined using a spatial convolution. We compare the properties of different kernels, studying a variety of geometries and assessing the impact of perturbations to the strictly periodic configuration. In Sect. 4, we discuss Taylor series approximations in the VAT, and in Sect. 5, we use the generalized volume averaging technique to study Stokes' flow in porous media, a standard problem which illustrates very well the mathematical issues. Finally, in Sect. 6, we provide a list of recommendations for the choice of the averaging operator and conclude.

2 Smoothness of the Averaged Fields: Example Problems

In this section, we study four example cases: polynomials embedded in a porous medium, highly disordered structures, hydrostatic equilibrium and Taylor series for the VAT. Our goal is to emphasize the problems generated by the standard definition of the averaging operator,

$$\langle \bullet \rangle_{\sqcap}^{f}\Big|_{\mathbf{x}} = \frac{1}{\left|\mathcal{V}^f\right|(\mathbf{x})} \int_{\mathcal{V}^f(\mathbf{x})} \bullet \mathrm{d}V, \tag{1}$$

where $\langle \bullet \rangle_{\sqcap}^{f}$ is the intrinsic phase average, $\mathcal{V}^f(\mathbf{x})$ the fluid part within the averaging set centered at $\mathbf{x}$ (see Fig. 1) and $\left|\mathcal{V}^f\right|(\mathbf{x}) = \int_{\mathcal{V}^f(\mathbf{x})} \mathrm{d}V$. The notation $\bullet|_{\mathbf{x}}$ describes the point,

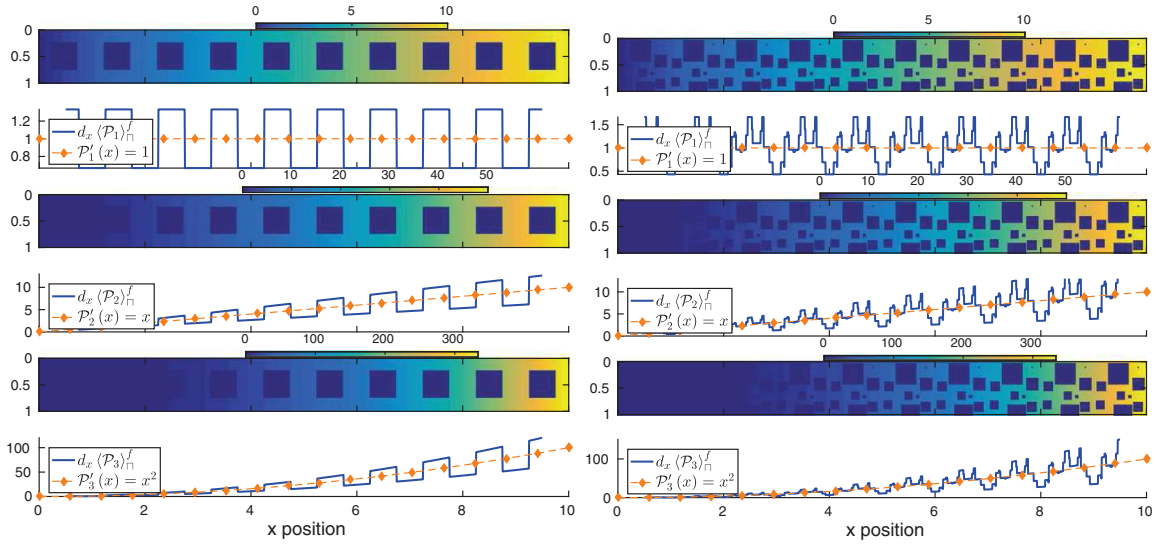

Fig. 2 Derivatives of the standard average of polynomial fields for ordered (*left-hand side*) and slightly disordered (*right-hand side*) periodic structures. The first rows represent the field $\chi^f \mathcal{P}_1$, with χ^f the fluid-phase indicator function, and the second rows are the derivatives $\mathrm{d}_x \langle \mathcal{P}_1 \rangle^f_\sqcap$ compared with the derivatives of the polynomial, $\mathcal{P}_1'$. The following rows are similar, but for $\mathcal{P}_2$ and $\mathcal{P}_3$. The width of the averaging window is $p = 1$ in each case. For simplicity, we only plot the average fields in the central part of the domain and avoid difficulties with average close to boundary conditions

x, at which the average field is evaluated. We also note $\mathcal{Y}$ the unit cell characterizing the periodic geometry, $\mathcal{Y}^f$ the fluid domain and $\partial\mathcal{Y}^{fs}$ the fluid–solid interface within the unit cell.

2.1 Polynomials

To illustrate how standard definitions of the averaging operator may yield anomalous behaviors of the average fields, we first consider the following polynomials, $\mathcal{P}_1(x) = x$, $\mathcal{P}_2(x) = \frac{1}{2}x^2$ and $\mathcal{P}_3(x) = \frac{1}{3}x^3$. These fields are embedded within a simple porous medium (Fig. 2), and we study the impact of the standard averaging operator, which in this case can be written as $\langle \bullet \rangle^f_\sqcap \Big|_x = \frac{1}{p\phi} \int_{x-\frac{p}{2}}^{x+\frac{p}{2}} \left(\int_0^1 \chi^f \bullet \mathrm{d}y \right) \mathrm{d}\xi$, with p the width of the averaging window, ϕ the porosity ($1/4$ in this case) and χ_f the fluid-phase indicator function (1 in the fluid and 0 in the solid). The symbol $\sqcap$ refers to the equivalent formulation using a convolution with a rectangular function, as will be clarified later on. Figure 2 shows that the derivatives of the average fields, $d_x \langle \mathcal{P}_1 \rangle^f_\sqcap$, $d_x \langle \mathcal{P}_2 \rangle^f_\sqcap$ and $d_x \langle \mathcal{P}_3 \rangle^f_\sqcap$, are discontinuous and strongly fluctuate compared to the smooth functions, $\mathcal{P}_1' = d_x\mathcal{P}_1 : x \to 1$, $\mathcal{P}_2' = d_x\mathcal{P}_2 : x \to x$ and $\mathcal{P}_3' = d_x\mathcal{P}_3 : x \to x^2$. The problem is clearly that the holes in the field due to the presence of the porous structure generate fluctuations in the average fields and that the standard definition of the averaging operator does not smooth these out properly.

2.2 Polynomials with a Highly Disordered Geometry and $\ell_p \ll \ell_u$

Here we ask the question of whether, and to what degree, some specific porous geometries can attenuate the problems generated by $\langle \bullet \rangle^f_\sqcap$. In Quintard and Whitaker (1994b, a), the authors showed that the problem is attenuated if the following two constraints are satisfied: (1) the medium is highly disordered and (2) the characteristic size of the pores (e.g., a correlation length for instance), ℓ_p, must be much smaller than the size of the unit cell, ℓ_u, i.e., $\ell_p \ll \ell_u$. In Fig. 3, we show that the fluctuations induced by $\langle \bullet \rangle^f_\sqcap$ do indeed decrease with ℓ_p for a

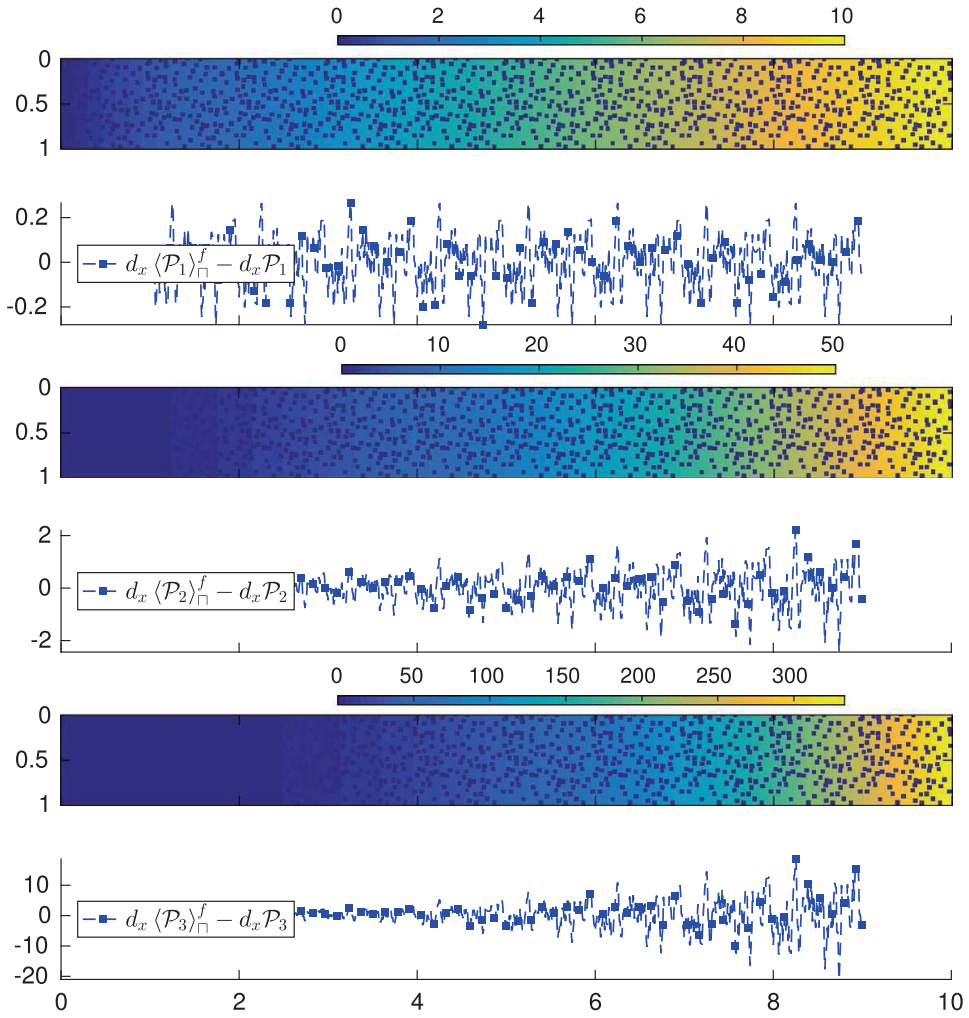

Fig. 3 Derivatives of the standard average of polynomial fields for a highly disordered periodic structure and with the pore size small compared to the unit cell. The first row represents the field $\chi^f \mathcal{P}_1$, with χ^f the fluid-phase indicator function, and the second row is the derivative $d_x \langle \mathcal{P}_1 \rangle^f_\sqcap$ compared with the derivative of the polynomial, $\mathcal{P}_1'$. The following rows are similar, but for $\mathcal{P}_2$ and $\mathcal{P}_3$. The width of the averaging window is $p = 1$

disordered geometry. However, we see that the discontinuities persist and that, even in this case, we cannot eliminate these completely, leaving us with the same fundamental issue.

2.3 Hydrostatic Equilibrium

To understand the implications for transport in porous media, we consider hydrostatic equilibrium in a porous medium, an example that was already discussed in detail in Quintard and Whitaker (1994a, b). Darcy's law in this configuration reads

$$-\frac{\mathbf{K}}{\mu} \cdot \left(\nabla \langle P \rangle^f_{\mathrm{D}} \Big|_{\mathbf{x}} - \rho \mathbf{g} \right) = 0, \tag{2}$$

so that

$$\nabla \langle P \rangle^f_{\mathrm{D}} \Big|_{\mathbf{x}} = \rho \mathbf{g}, \tag{3}$$

with P the pressure, the density ρ and the viscosity μ considered constant and $\mathbf{g}$ the gravitational acceleration. On the other hand, the hydrostatic pressure solves the following equation at the microscale,

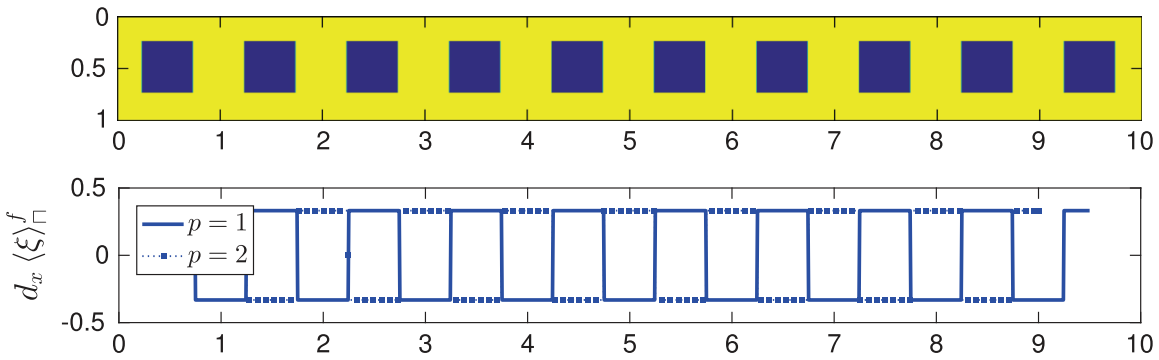

Fig. 4 Fluctuations of $d_x \langle \xi \rangle_\sqcap^f$ for a model porous medium. The first row represents the porous structure and the following one corresponds to different sizes of the averaging window, $p = 1$ and 2

$$\nabla P(\mathbf{x}) = \rho \mathbf{g}. \tag{4}$$

The analytical solution to this problem is therefore

$$P(\mathbf{x}) = P_0 + \mathbf{x} \cdot \rho \mathbf{g}, \tag{5}$$

where $\mathbf{x}$ is the position vector and P_0 is, for simplicity, a reference pressure at $\mathbf{x} = 0$. To compare this with the result of Darcy's law, we average the analytical solution in space with the standard definition of the averaging operator Eq. 1. We obtain

$$\langle P \rangle_\sqcap |_{\mathbf{x}}^f = P_0 + \left(\mathbf{x} + \langle \boldsymbol{\xi} \rangle_\sqcap |_{\mathbf{x}}^f \right) \cdot \rho \mathbf{g}, \tag{6}$$

evaluated at point $\mathbf{x}$ and $\boldsymbol{\xi}$ is the vector pointing from the center, $\mathbf{x}$, to points within the averaging volume (see Fig. 1). This yields

$$\nabla \langle P \rangle_\sqcap^f \Big|_{\mathbf{x}} = \left(\mathbf{I} + \nabla \langle \boldsymbol{\xi} \rangle_\sqcap^f \Big|_{\mathbf{x}} \right) \cdot \rho \mathbf{g}. \tag{7}$$

We therefore obtain a different form of the pressure gradient depending on the calculation method, the difference being

$$\nabla \langle P \rangle_\sqcap^f \Big|_{\mathbf{x}} - \nabla \langle P \rangle_{\mathrm{D}}^f \Big|_{\mathbf{x}} = \nabla \langle \boldsymbol{\xi} \rangle_\sqcap^f \Big|_{\mathbf{x}} \cdot \rho \mathbf{g}. \tag{8}$$

What is the origin and extent of this difference? To evaluate this, we calculate the value of $d_x \langle \xi \rangle_\sqcap^f \Big|_x$ for an ordered periodic porous structure in the configuration presented in Fig. 4, i.e., a quasi-one-dimensional situation. The averaging volume is simply defined as the moving spatial average over the volume of the unit cell, as in Eq. 1. For this structure, we see that $\left| d_x \langle \xi \rangle_\sqcap^f \Big|_x \right| = \mathcal{O}(1)$ and cannot be neglected. We further show in Fig. 4 that the width of the averaging window does not impact the norm of the fluctuations, as was suggested in Howes and Whitaker (1985), but only its phase ($\frac{\pi}{2}$ between p even and odd). In fact, the use of an averaging volume of different shape, for instance a cylinder as proposed in Howes and Whitaker (1985), does not help either, as shown in Quintard and Whitaker (1994b). Therefore, we conclude that the standard averaging operator is incompatible with the usual form of Darcy's law.

We can, however, overcome this issue and obtain a corrected pressure, $\langle P \rangle_c^f$, defined by

$$\langle P \rangle_c^f \Big|_{\mathbf{x}} = \langle P \rangle_\sqcap^f \Big|_{\mathbf{x}} - \langle \boldsymbol{\xi} \rangle_\sqcap^f \Big|_{\mathbf{x}} \cdot \left(\mathbf{I} + \nabla \langle \boldsymbol{\xi} \rangle_\sqcap^f \Big|_{\mathbf{x}} \right)^{-1} \cdot \nabla \langle P \rangle_\sqcap^f \Big|_{\mathbf{x}}, \tag{9}$$

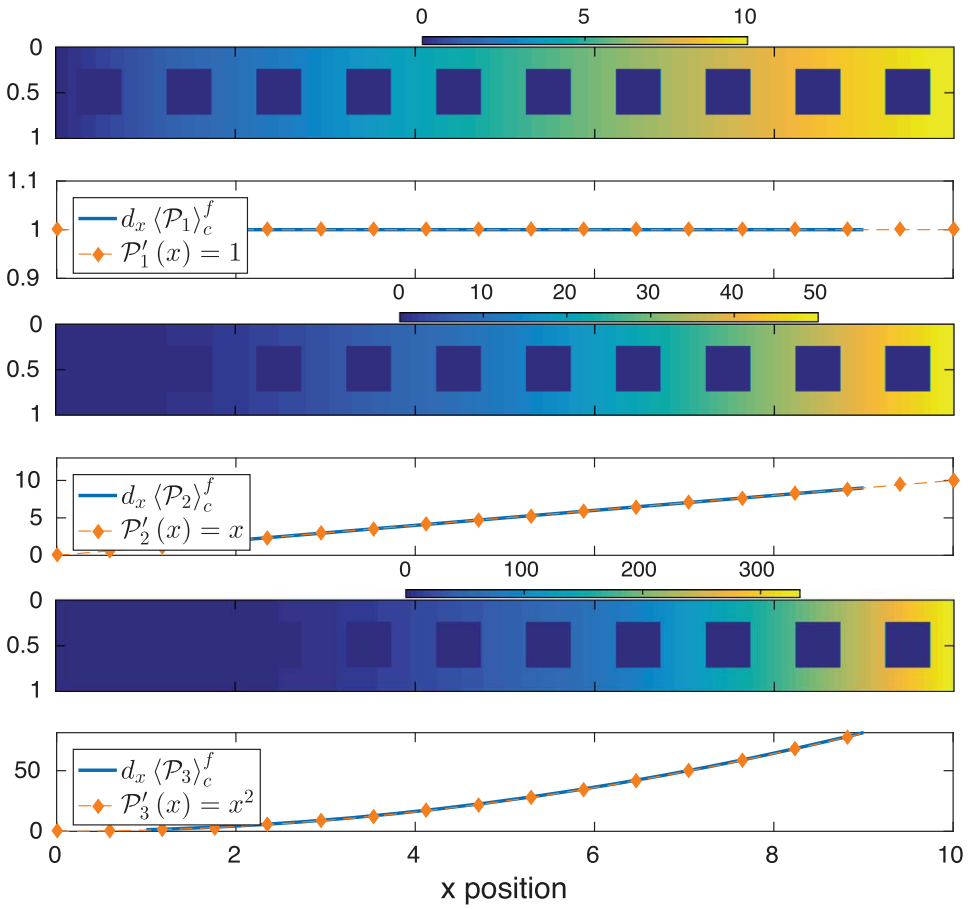

Fig. 5 Corrected derivatives of the average of polynomial fields. The first row represents the field $\chi^f \mathcal{P}_1$, and the second row is the derivative $d_x \langle \mathcal{P}_1 \rangle_c^f = \left(1 + d_x \langle \xi \rangle_\sqcap^f\right)^{-1} d_x \langle \mathcal{P}_1 \rangle_\sqcap^f$ compared to $\mathcal{P}_1'$. The following rows are similar, but for $\mathcal{P}_2$ and $\mathcal{P}_3$. These show that the regularization by $\left(1 + d_x \langle \xi \rangle_\sqcap^f\right)^{-1}$ regularizes the gradients

which yields the gradient

$$\nabla \langle P \rangle_c^f \Big|_{\mathbf{x}} = \left(\mathbf{I} + \nabla \langle \boldsymbol{\xi} \rangle_\sqcap^f \Big|_{\mathbf{x}}\right)^{-1} \cdot \nabla \langle P \rangle_\sqcap^f \Big|_{\mathbf{x}} . \tag{10}$$

In Fig. 5, we see that the regularization using $\left(\mathbf{I} + \nabla \langle \boldsymbol{\xi} \rangle_\sqcap^f \Big|_{\mathbf{x}}\right)$ smoothes out the polynomial fields by eliminating the fluctuations, so that we can use this in the VAT to obtain a corrected hydrostatic form of Darcy's law,

$$0 = -\frac{\mathbf{K}}{\mu} \cdot \left(\nabla \langle P \rangle_c^f \Big|_{\mathbf{x}} - \rho \mathbf{g}\right). \tag{11}$$

Another solution consists in writing Darcy's law as

$$0 = -\frac{\mathbf{K}}{\mu} \cdot \nabla \left\langle P^* \right\rangle_\sqcap^f \Big|_{\mathbf{x}} , \tag{12}$$

with $P^*(\mathbf{x}) = P(\mathbf{x}) - \mathbf{x} \cdot \rho \mathbf{g}$. These regularizations *a posteriori*, however, are only tricks that do not address the fundamental issue. In particular, we used the notation $\langle P \rangle_c^f$, which suggests that this field can be obtained directly from a proper definition of the averaging operator. What is the operational significance of $\langle P \rangle_c^f$? As we will see, there is a much more generic way to deal with this issue by defining the average using spatial convolutions.

2.4 Taylor Series

The VAT is a perturbation method based on a spatial perturbation in the form,

$$g = \langle g \rangle_{\sqcap}^{f}\Big|_{\mathbf{x}} + \tilde{g}\,(\mathbf{x})\,. \tag{13}$$

In using this decomposition, one often obtains successive averages of microscale fields. For instance, to obtain the condition $\langle \tilde{g} \rangle_{\sqcap}^{f}\Big|_{\mathbf{x}} \simeq 0$ which is used systematically in the VAT, we have to average Eq. 13 as

$$\langle g \rangle_{\sqcap}^{f}\Big|_{\mathbf{x}} = \left\langle \langle g \rangle_{\sqcap}^{f}\Big|_{\mathbf{r}} \right\rangle_{\sqcap}^{f}\Big|_{\mathbf{x}} + \langle \tilde{g} \rangle_{\sqcap}^{f}\Big|_{\mathbf{x}}\,. \tag{14}$$

Then, in order to evaluate $\left\langle \langle g \rangle_{\sqcap}^{f}\Big|_{\mathbf{r}} \right\rangle_{\sqcap}^{f}\Big|_{\mathbf{x}}$, we go on to use Taylor series to approximate $\langle g \rangle_{\sqcap}^{f}\Big|_{\mathbf{r}}$ about $\mathbf{x}$. The order of this Taylor series depends on the problem considered, but in general we must match the order of the Taylor series with that of the closure, i.e., the approximate form of the perturbation $\tilde{g}$. To do so, however, the Taylor series must exist. For a first-order Taylor series, we would need $\langle g \rangle_{\sqcap}^{f} \in C^1\,(\mathbb{R}^n)$, which is not the case for a periodic geometry. Hence, we cannot use such Taylor series with the standard definition of the average.

3 Generalized Averaging Using Spatial Convolutions

As discussed in Introduction, the primary goal of the spatial averaging operator is to filter out high-frequency spatial fluctuations. In this sense, the averaging operator defined as

$$\langle \bullet \rangle_{\sqcap}^{f}\Big|_{\mathbf{x}} = \frac{1}{\left|\mathcal{V}^f\right|(\mathbf{x})} \int_{\mathcal{V}^f(\mathbf{x})} \bullet \mathrm{d}V = \frac{1}{\left|\mathcal{V}^f\right|(\mathbf{x})} \int_{\mathcal{V}(\mathbf{x})} \chi^f \bullet \mathrm{d}V, \tag{15}$$

with χ_f the fluid-phase indicator function, is not performing well: it fails to filter out part of the fluctuations due to the porous structure. By changing the definition of the spatial averaging operator, we will see that we can attenuate and even eliminate these fluctuations in some cases.

3.1 Definition of the Generalized Average

In order to generalize the notion of averaging, we define it as a spatial convolution as was done in Marle (1982), Quintard and Whitaker (1994a, b). For a field g in the fluid phase f, this reads

$$\langle g \rangle|_{\mathbf{x}} = \int_{\mathbb{R}^n} m\,(\mathbf{x}-\mathbf{r})\,\chi^f\,(\mathbf{r})\,g\,(\mathbf{r})\,\mathrm{d}\mathbf{r} = m * \left(\chi^f g\right)\Big|_{\mathbf{x}}, \tag{16}$$

with m a normalized kernel, $\int_{\mathbb{R}^n} m\,(\mathbf{r})\,\mathrm{d}\mathbf{r} = 1$, and χ^f the fluid-phase indicator function, whose value is 1 in the fluid phase and 0 otherwise. The porosity is $\phi = \langle 1 \rangle|_{\mathbf{x}} = m * \chi_f\,(\mathbf{x})$, and the intrinsic average (with the upper script f) is

$$\langle g \rangle^f\Big|_{\mathbf{x}} = \frac{m * \left(\chi^f g\right)}{m * \chi^f}\Big|_{\mathbf{x}} = \frac{m * \left(\chi^f g\right)}{\phi}\Big|_{\mathbf{x}}, \tag{17}$$

so that $\langle 1 \rangle^f \big|_{\mathbf{x}} = 1$. This definition using a convolution is associated with a very well-established mathematical background (convolutions in $L^1(\mathbb{R}^n)$ and $L^2(\mathbb{R}^n)$, distributions, Fourier transforms), for which it is relatively easy to extract physically relevant properties, in particular regarding the smoothness of the average fields (see for instance in Schwartz (1978), Gray et al. (1993), Strichartz (1994)).

Here the kernel m has the following properties:

1. m acts as a low-pass filter,
2. m has symmetries such that $m\left(\begin{bmatrix} x_1 \\ \vdots \\ -x_i \\ \vdots \\ x_n \end{bmatrix}\right) = m\left(\begin{bmatrix} x_1 \\ \vdots \\ x_i \\ \vdots \\ x_n \end{bmatrix}\right)$ for any value of $i \in [\![1, n]\!]$.
3. For simplicity, we consider that the unit cell is a n-dimensional unit cube $[0, 1]^n$ so that, in general, m can be written as $m = \prod_{i=1}^{n} f(x_i)$.

Other properties, which are more specific to the VAT, we discuss later on.

3.2 Generic Positive Kernels

The first kernel that we consider is a n-dimensional rectangular function $m_\sqcap$ defined as the product

$$m_\sqcap(\mathbf{x}) = \prod_{i=1}^{n} R(x_i), \tag{18}$$

with $\mathbf{x} = (x_1 \cdots x_n)^\mathsf{T}$ and the one-dimensional rectangular function defined as

$$R(t) = \begin{cases} \frac{1}{p_\sqcap} & \text{if } |t| < \frac{p_\sqcap}{2}, \\ \frac{1}{2p_\sqcap} & \text{if } |t| = \frac{p_\sqcap}{2}, \\ 0 & \text{if } |t| > \frac{p_\sqcap}{2}. \end{cases} \tag{19}$$

This allows us to define the corresponding *phase* average, $\langle g \rangle_\sqcap \big|_{\mathbf{x}} = m_\sqcap * (\chi_f g)(\mathbf{x})$. We can further write the *intrinsic* average of any function g with the upper script f as

$$\langle g \rangle_\sqcap^f \Big|_{\mathbf{x}} = \frac{m_\sqcap * (\chi_f g)}{m_\sqcap * \chi_f}(\mathbf{x}), \tag{20}$$

This definition of the average is the one used in Sect. 2.

With $m_\sqcap$, we can define the n-dimensional triangular function as

$$m_\wedge(\mathbf{x}) = m_\sqcap * m_\sqcap(\mathbf{x}), \tag{21}$$

This may also be written as

$$m_\wedge(\mathbf{x}) = \prod_{i=1}^{n} T(x_i), \tag{22}$$

with

$$T(t) = \begin{cases} \frac{2}{p_\wedge}\left(1 - \frac{2}{p_\wedge}|t|\right) & \text{if } |t| < \frac{p_\wedge}{2}, \\ 0 & \text{if } |t| \geq \frac{p_\wedge}{2}, \end{cases} \tag{23}$$

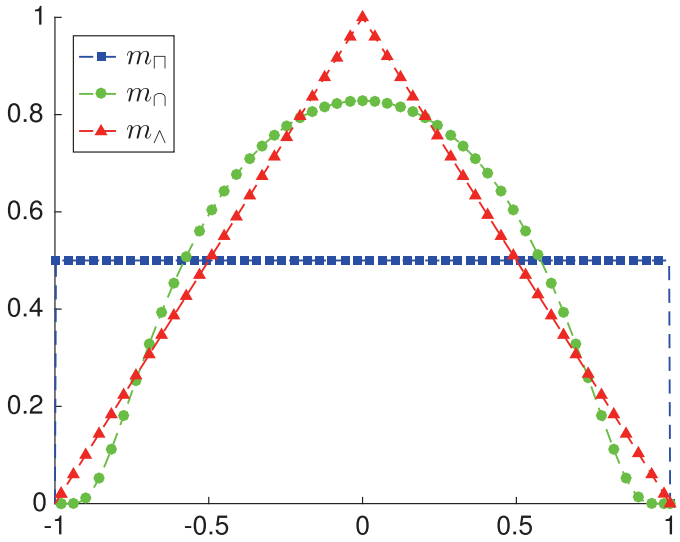

Fig. 6 Example one-dimensional kernels used in the spatial convolution. $m_\sqcap$, $m_\cap$ and $m_\wedge$ are, respectively, *rectangular*, *mollifier* (as defined in Eq. 25) and *triangular* functions

with $p_\wedge = 2p_\sqcap$. The corresponding intrinsic average reads

$$\langle g \rangle_\wedge^f \Big|_{\mathbf{x}} = \frac{m_\wedge * \left(\chi_f g\right)}{m_\wedge * \chi_f} (\mathbf{x}) . \tag{24}$$

We also consider a mollifier as a kernel for the convolution. By definition, a mollifier η is a smooth function on $\mathbb{R}^n$ which is compactly supported and satisfies $\int_{\mathbb{R}^n} \eta(\mathbf{r}) \, \mathrm{d}\mathbf{r} = 1$ and $\lim_{\varepsilon \to 0} \varepsilon^{-n} \eta\left(\frac{\mathbf{x}}{\varepsilon}\right) = \delta(\mathbf{x})$, with $\delta(\mathbf{x})$ a Dirac delta. This makes it a perfect fit for use as a spatial filter in the VAT and we consider the following mollifier,

$$m_\cap(\mathbf{x}) = \begin{cases} \frac{1}{C_{n,\cap}} \exp\left(-\frac{(p/2)^2}{(p/2)^2 - |\mathbf{x}|^2}\right) & \text{if } |\mathbf{x}| < \frac{p_\cap}{2}, \\ 0 & \text{if } |\mathbf{x}| \geq \frac{p_\cap}{2}, \end{cases} \tag{25}$$

with $C_{n,\cap}$ defined so that $\int_{\mathbb{R}^n} m_\cap(\mathbf{r}) \, \mathrm{d}\mathbf{r} = 1$. A one-dimensional version of $m_\sqcap$, $m_\wedge$ and $m_\cap$ is plotted in Fig. 6.

We now study the properties of these different kernels, which are as follows.

3.2.1 Rectangular Kernel

- *Smoothness* one of the main problems with the rectangular kernel is that it is discontinuous and may yield derivatives of the average that do not exist everywhere (Howes and Whitaker 1985). In fact, we have $\langle g \rangle_\sqcap^f \in C_c^0(\mathbb{R}^n)$ (without entering mathematical details, this requires that $m_\sqcap$ and $\chi^f g$ are both in $L^2(\mathbb{R}^n)$) and the derivative is discontinuous at several points, as shown in Fig. 9 for polynomials.
- *Fluctuations* the rectangular kernel does not filter out the fluctuations induced by the geometry of the porous structure, as shown in Fig. 7. We can assess the situation analytically considering the one-dimensional derivative

$$d_x \langle \mathcal{P}_1 \rangle_\sqcap^f = \frac{m_\sqcap * d_x\left(\chi_f \mathcal{P}_1\right)}{m_\sqcap * \chi_f} (x) . \tag{26}$$

  Expressing the derivative of the product as $d_x\left(\chi_f \mathcal{P}_1\right) = \chi_f \left(d_x \mathcal{P}_1\right) + \left(d_x \chi_f\right) \mathcal{P}_1$, we obtain

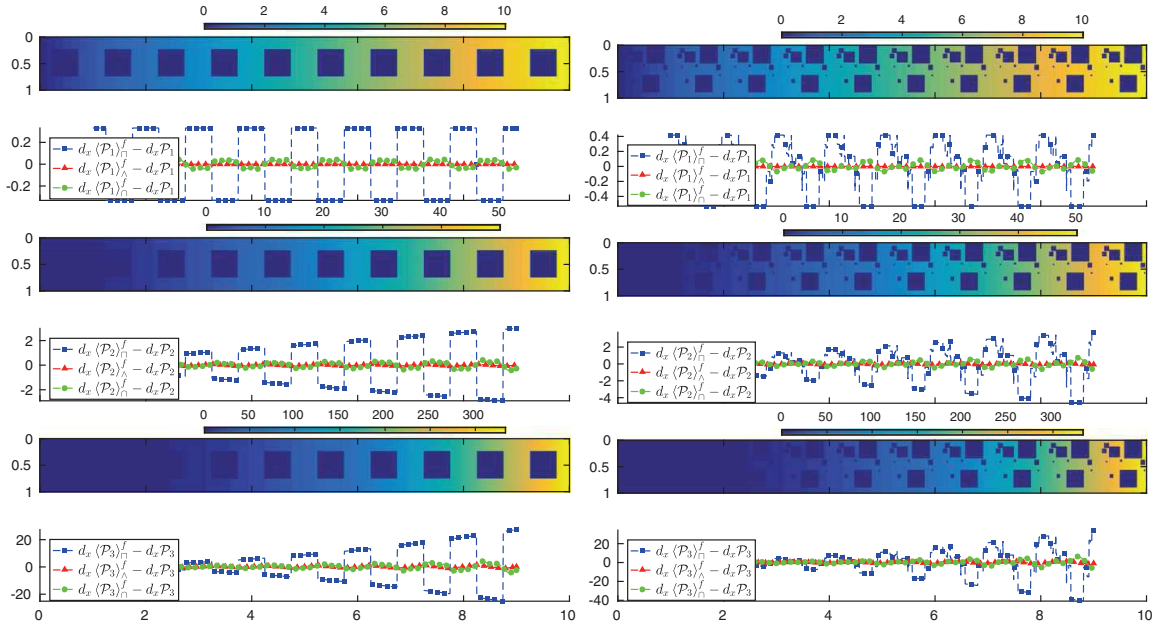

Fig. 7 Derivatives of the average of polynomial fields obtained for ordered (*left-hand side*) and slightly disordered (*right-hand side*) periodic structures. The first rows represent the field $\chi^f \mathcal{P}_1$, and the second rows are the derivatives $d_x \langle \mathcal{P}_1 \rangle^f_\sqcap - d_x \mathcal{P}_1$, $d_x \langle \mathcal{P}_1 \rangle^f_\cap - d_x \mathcal{P}_1$ and $d_x \langle \mathcal{P}_1 \rangle^f_\wedge - d_x \mathcal{P}_1$. The following rows are similar, but for $\mathcal{P}_2$ and $\mathcal{P}_3$. The width of the averaging window is $p = 2$ for each case

$$d_x \langle \mathcal{P}_1 \rangle^f_\sqcap = \langle d_x \mathcal{P}_1 \rangle^f_\sqcap + \frac{m_\sqcap * \left[\left(d_x \chi_f \right) \mathcal{P}_1 \right]}{m_\sqcap * \chi_f} (x) \,. \tag{27}$$

Without going further, we see that the perturbation from $\langle d_x \mathcal{P}_1 \rangle^f_\sqcap = 1$ is induced, here, by the geometry $d_x \chi_f$.

– *Effect on a periodic function* if a is periodic, then the size of the averaging window does not affect the result if $p \in \mathbb{N}^{+*}$. We therefore have $\langle a \rangle^f_{\sqcap,\ p=1} = \langle a \rangle^f_{\sqcap,\ p=2} = \cdots = \langle a \rangle^f_{\sqcap,\ p=k}$, for any value of $k \in \mathbb{N}^{+*}$.
– *Quasiperiodicity* we present results for two quasiperiodic structures in Fig. 8: one with linear variation of the porosity and the other one with a random displacement of the solid within each unit cell. We see that the rectangular kernel fails again to filter out the fluctuations in both cases.

3.2.2 Triangular Kernel

– *Smoothness* first-order derivatives with the triangular function are well defined, $\langle g \rangle^f_\wedge \in C^1(\mathbb{R}^n)$ for $\chi^f g \in L^2(\mathbb{R}^n)$. Figure 7 shows these behaviors for the first-order derivatives and model porous structures.
– *Fluctuations* the triangular kernel is much better than $m_\sqcap$ at filtering the fluctuations induced by the porous medium geometry, as shown in Fig. 7. For $\mathcal{P}_1$, it smoothes out the field perfectly, while doing a much better job than the rectangular kernel for higher-order polynomials.
– *Effect on a periodic function* if a is periodic and $\frac{p_\wedge}{2} \in \mathbb{N}^{+*}$ then

$$\langle a \rangle^f_\wedge = \langle a \rangle^f_\sqcap \,. \tag{28}$$

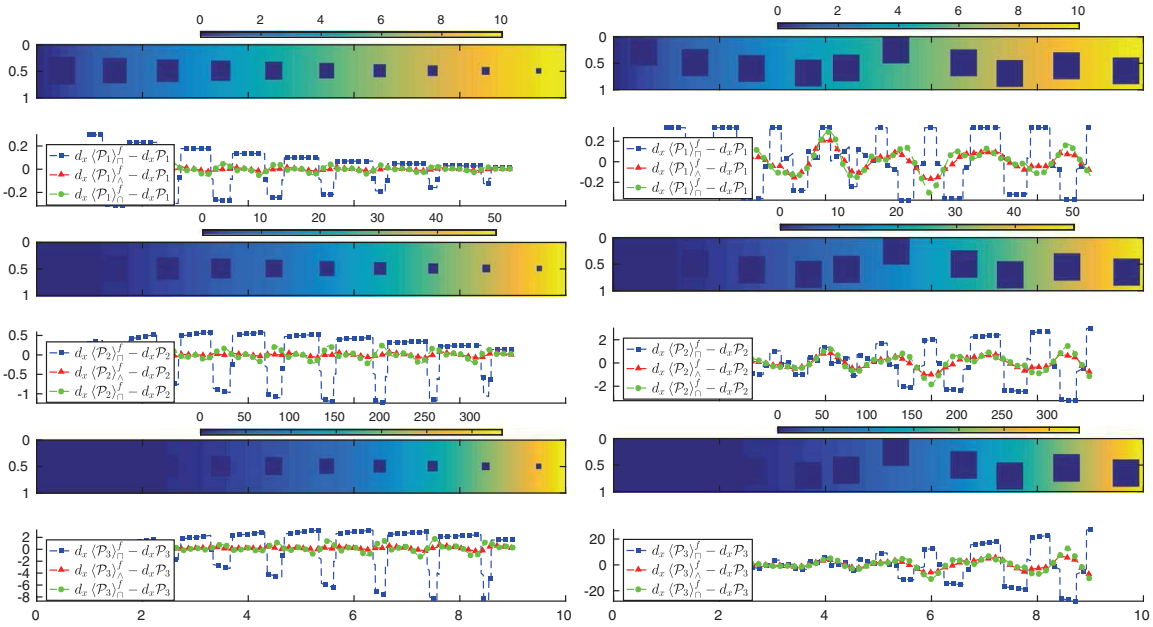

Fig. 8 Derivatives of the average of polynomial fields obtained for quasiperiodic structures, with a linear variation of the porosity (*left-hand side*) and a random displacement of the solid phase within each unit cell (*right-hand side*). The first rows represent the field $\chi^f \mathcal{P}_1$, and the second rows are the derivatives $d_x \langle \mathcal{P}_1 \rangle_{\sqcap}^f - d_x \mathcal{P}_1$, $d_x \langle \mathcal{P}_1 \rangle_{\cap}^f - d_x \mathcal{P}_1$ and $d_x \langle \mathcal{P}_1 \rangle_{\wedge}^f - d_x \mathcal{P}_1$. The following rows are similar, but for $\mathcal{P}_2$ and $\mathcal{P}_3$. The width of the averaging window is $p = 2$ for each case

This is straightforward considering $m_\wedge = m_\sqcap * m_\sqcap$, the associativity of the convolution product and the fact that $\langle a \rangle_\sqcap^f$ is constant. Further, $\langle a \rangle_\sqcap^f$ can be calculated with a unit averaging window since we have seen that p is unimportant if a is periodic. Why is this interesting? An important part of the VAT is the use of closure variables. These closure variables are generally expressed as solutions of a closure problem in a single unit cell with periodic boundary conditions. Effective parameters that appear in the macroscale average equations are then expressed as volume integrals of these closure variables. The relation $\langle a \rangle_\wedge = \langle a \rangle_\sqcap$ allows us to use the triangular kernel for averaging while still working with a single unit cell to calculate effective parameters by averaging with the rectangular kernel. This important result can be used to unite results from homogenization theory and VAT as illustrated in Quintard and Whitaker (1994), justifying the resolution of closure problems on a single unit cell for the periodic case.

– *Quasiperiodicity* in Fig. 8, we see that the triangular kernel partly filters out the fluctuations induced by a linear variation of the porosity. In the case of the random displacement, however, we see in Fig. 9 that the width of the averaging window plays an important role to capture the disorder and that the accuracy can be made better by increasing $p_\wedge$. In both cases, however, $d_x \langle g \rangle_\wedge^f$ is only $C^0(\mathbb{R}^n)$.

3.2.3 Mollifier Kernel

– *Smoothness* the mollifier is particularly interesting because, contrary to the rectangular and triangular functions, it is $C_c^\infty(\mathbb{R}^n)$ so that $\langle g \rangle_\cap^f \in C^\infty(\mathbb{R}^n)$. Figure 7 shows this for the first-order derivatives of polynomials and model porous structures.

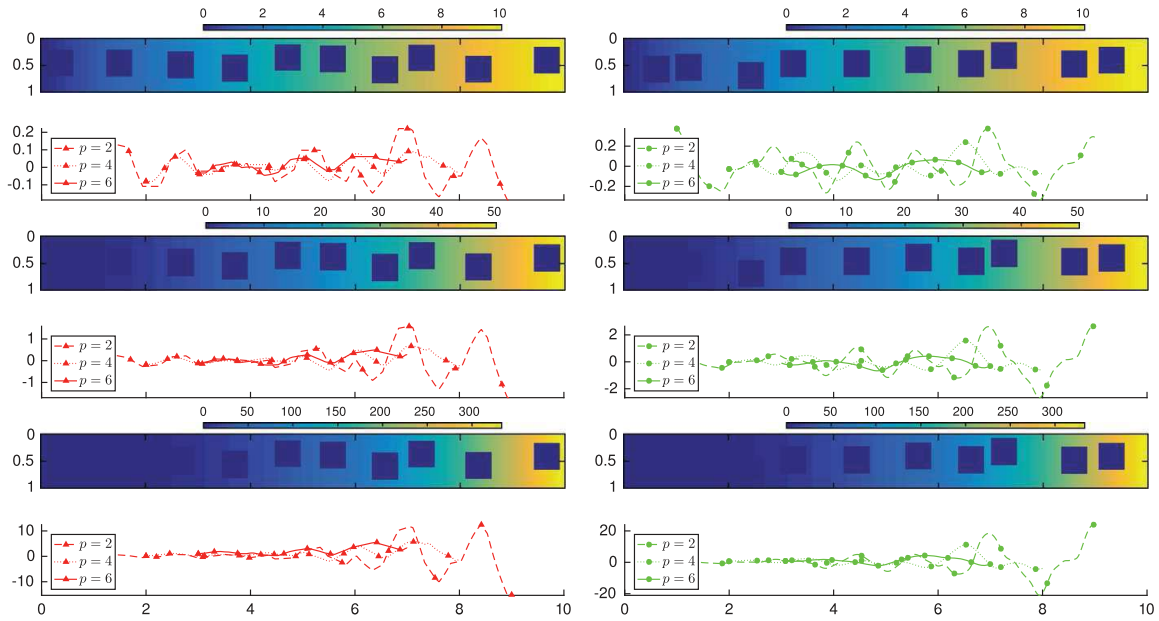

Fig. 9 Derivatives of the average of polynomial fields obtained for different width of the averaging window with the *triangular* (*left-hand side*) and *mollifier* (*right-hand side*) kernels. The first rows represent the field $\chi^f \mathcal{P}_1$, and the second rows are the derivatives $d_x \langle \mathcal{P}_1 \rangle^f_\wedge - d_x \mathcal{P}_1$ and $d_x \langle \mathcal{P}_1 \rangle^f_\cap - d_x \mathcal{P}_1$ for $p = 2,\ 4,$ and 6. The following rows are similar, but for $\mathcal{P}_2$ and $\mathcal{P}_3$ **a** $m_\wedge$ **b** $m_\cap$

- *Fluctuations* as shown in Fig. 7, the mollifier is efficient at filtering out the fluctuations induced by the porous geometry. Further, these fluctuations decrease with an increasing width of averaging window, $p_\cap$ (see, for example, Figs. 7 and 10).
- *Effect on a periodic function* if a is periodic then

$$\langle a \rangle^f_\cap \neq \langle a \rangle^f_\sqcap . \tag{29}$$

- *Quasiperiodicity* in Fig. 8, we see that the mollifier partly filters out the fluctuations induced by a linear variation of the porosity, with a similar amplitude to that of the triangular kernel. As for $m_\wedge$, we see in Fig. 9 that, for the random displacements, the width of the averaging window plays an important role to capture the disorder and that the accuracy can be made better by increasing $p_\cap$. In both cases, we further see that $d_x \langle g \rangle^f_\cap$ is smooth.

3.2.4 Hydrostatic Case

Getting back to transport in porous media, we consider here the situation presented in Sect. 2.3 and variations of the term $\nabla \langle \boldsymbol{\xi} \rangle^f_\sqcap \Big|_{\mathbf{x}}$. In Fig. 10, we see that the rectangular function induces strong fluctuations and discontinuities of $d_x \langle \xi \rangle^f_\sqcap$ in the ordered and disordered geometries. On the other hand, the triangular function does a perfect job, with no fluctuations, while the mollifier smoothes the fields out and considerably reduces the amplitude of the fluctuations. For quasiperiodic geometries, as shown in Fig. 10, we see again that the rectangular kernel induces strong fluctuations and discontinuities, while the triangular and mollifier are much more efficient.

3.3 Compositions of Positive Kernels

Here, we compose the basic kernels presented above to combine their advantages.

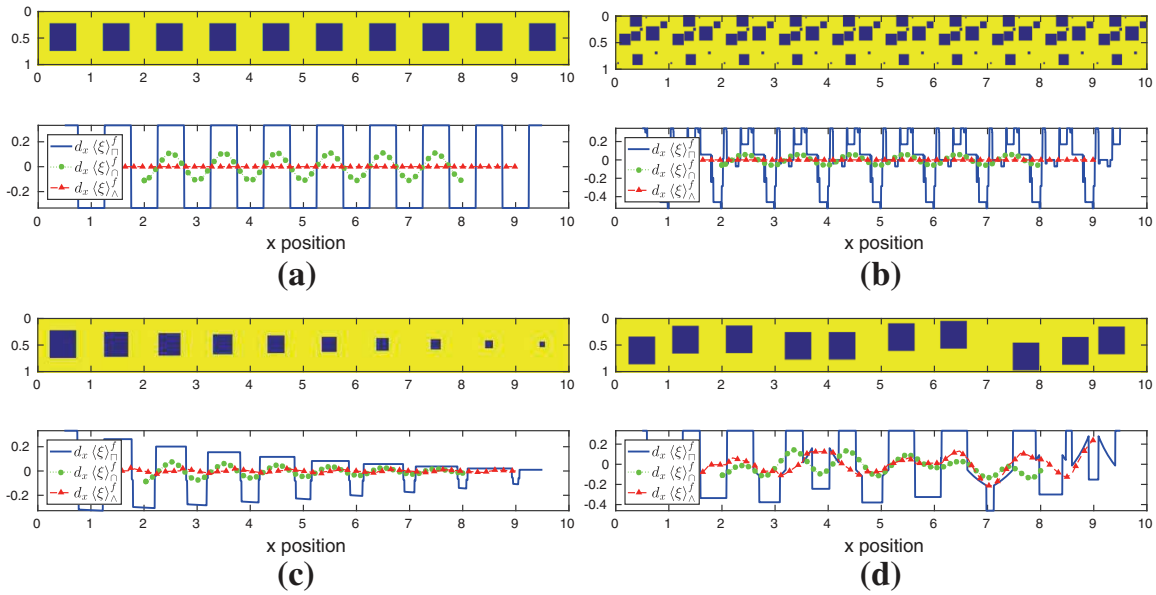

Fig. 10 Fluctuations of $d_x \langle \xi \rangle^f$ for a model porous medium. The first rows represent the porous structures for **a** ordered, **b** slightly disordered, **c** a linear variation of the porosity and **d** a random displacement of the solid phase within each unit cell. The second rows correspond to $d_x \langle \xi \rangle^f$ obtained using different averaging kernels, $m = m_\sqcap,\ m_\cap,$ and $m_\wedge$

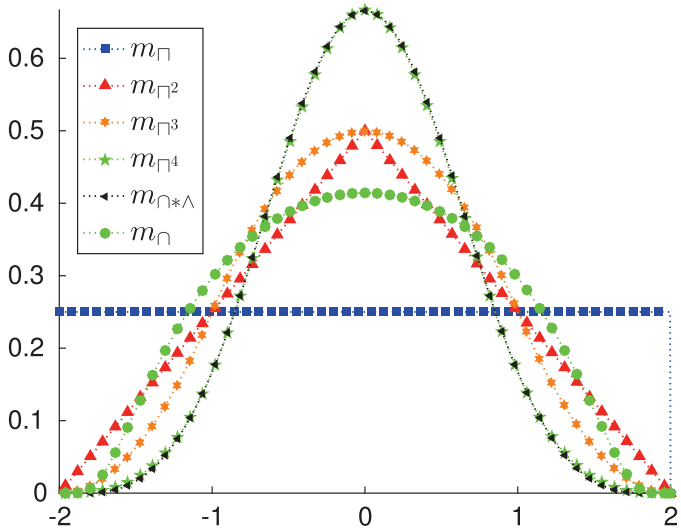

Fig. 11 Example one-dimensional kernels used in the spatial convolution

3.3.1 Successive Convolutions of $m_\sqcap$: Cardinal B-splines

We can obtain a sequence of kernels by repeating convolutions of $m_\sqcap$. We write

$$m_{\sqcap^{q>1}} = \underbrace{m_\sqcap * \cdots * m_\sqcap}_{\text{q times}}, \tag{30}$$

where $q \in \mathbb{N}^{+*}$, which is also known as the $(q-1)$th cardinal B-spline function (usually translated to $\mathbb{R}^+$). Note the special case $m_\wedge = m_{\sqcap^2}$. Such kernels were already used up to $q = 2$ in Quintard and Whitaker (1994b) and $q = 3$ in d'Hueppe et al. (2011) to deal with an interface between a fluid and a porous medium. Example kernels are plotted in Fig. 11. This kernel has the following properties.

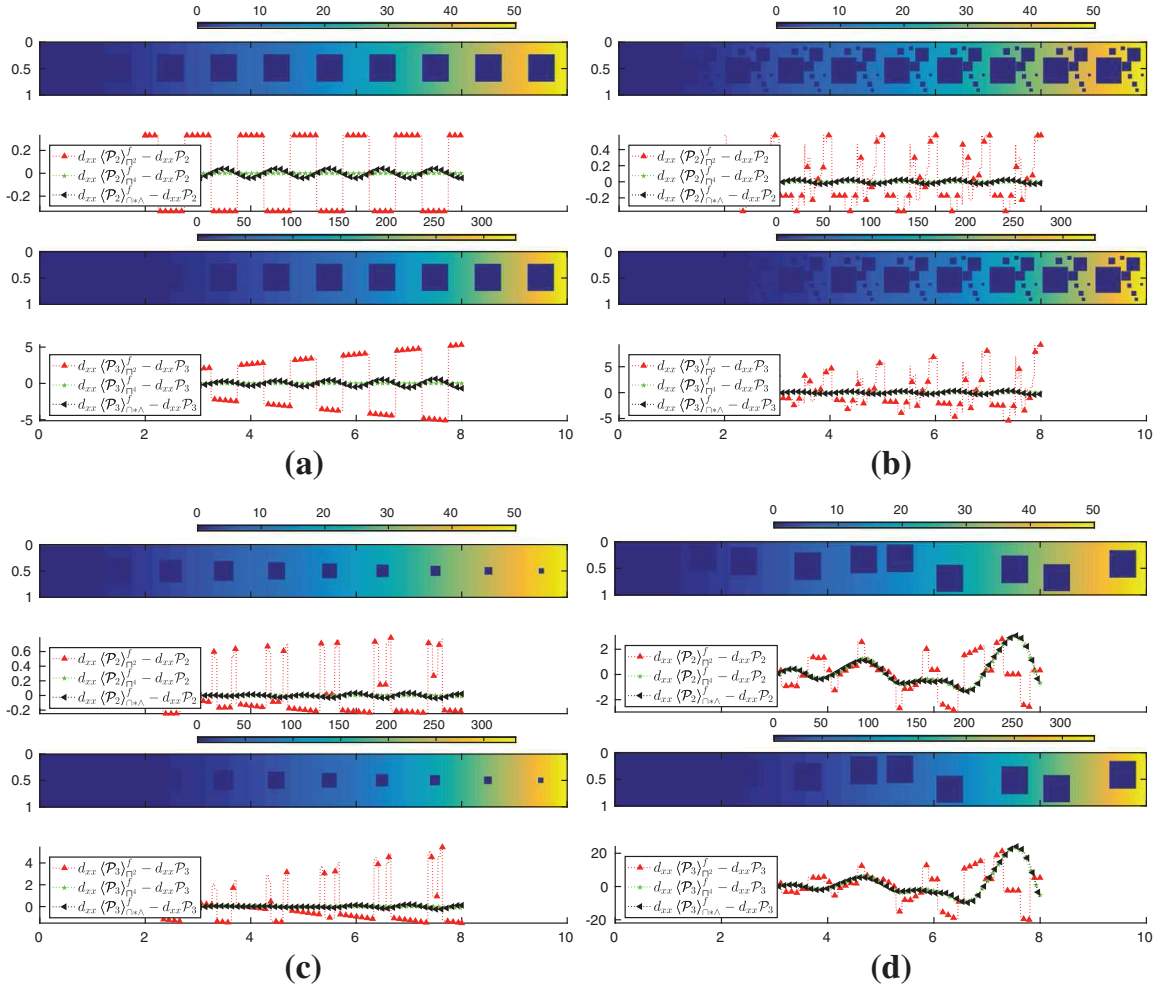

Fig. 12 Second-order derivatives of the average of polynomial fields obtained for **a** ordered, **b** disordered, **c** a linear variation of the porosity and **d** a random displacement of the solid phase within each unit cell. The first rows represent the field $\chi^f \mathcal{P}_2$, and the second rows are the derivatives $d_x \langle \mathcal{P}_2 \rangle^f_{\sqcap^2} - d_x \mathcal{P}_2$, $d_x \langle \mathcal{P}_2 \rangle^f_{\sqcap^3} - d_x \mathcal{P}_2$ and $d_x \langle \mathcal{P}_2 \rangle^f_{\cap * \wedge} - d_x \mathcal{P}_2$. The following rows are similar, but for $\mathcal{P}_3$. The width of the averaging window is $p = 4$ for each case

- *Smoothness* $m_{\sqcap^q} \in C_c^{q-1}(\mathbb{R}^n)$ for $q \geq 1$ and $\langle g \rangle^f_{\sqcap^q} \in C^q(\mathbb{R}^n)$ for $\chi^f g \in L^2(\mathbb{R}^n)$. Therefore, we can choose the smoothness of the average field by changing q. Figure 12 shows this for the second-order derivatives and model porous structures.
- *Fluctuations* $m_{\sqcap^{q>1}}$ is very efficient at filtering out the fluctuations induced by the porous medium geometry, as shown in Fig. 12. We will see in Sect. 4 that we need q strictly larger than the order of the polynomial for the filtering to remain efficient.
- *Effect on a periodic function* the width of the averaging window, $p_{\sqcap^q}$, is here fixed by the number of convolutions and the window of the original rectangular function $p_\sqcap$, so that $p_{\sqcap^q} = q p_\sqcap$. If a is periodic and $p_\sqcap = 1$, then

$$\langle a \rangle^f_{\sqcap^q} = \langle a \rangle^f_\sqcap . \tag{31}$$

  This gives $m_{\sqcap^{q>1}}$ the same advantage as $m_\wedge$ for the calculation of effective parameters on a single unit cell.
- *Quasiperiodicity* as shown in Fig. 12, $m_{\sqcap^q}$ gains in accuracy with increasing q for the linear variation, while q does not impact much the results for the random perturbations (rather p does as discussed for the other generic kernels).

– *Asymptotic behavior* at fixed value of $p_{\sqcap} = 1$, $m_{\sqcap^q}$ tends toward a Gaussian in the limit $q \to \infty$ (with also $p_{\sqcap^q} \to \infty$).

3.3.2 Kernels Built as Mixed Convolution of $m_{\cap}$ and $m_{\sqcap}$

We can mix the kernels to obtain special properties. For instance, we can convolve $m_{\cap}$ with $m_{\sqcap^q}$ as

$$m_{\cap * \sqcap^q} = \frac{1}{C_{n,\cap * \sqcap^q}} m_{\cap} * m_{\sqcap^q}, \tag{32}$$

where $C_{n,\cap * \sqcap^q}$ is a normalization constant and $q \in \mathbb{N}^+$. The advantage of this kernel is that it combines the smoothness of $m_{\cap}$ with the property that $\langle a \rangle^f_{\sqcap^q} = \langle a \rangle^f_{\sqcap}$ for a periodic. The width of the averaging window is $p_{\cap * \sqcap^q} = p_{\cap} + q p_{\sqcap}$. For simplicity, we consider here only the special case

$$m_{\cap * \sqcap^2} = m_{\cap * \wedge}, \tag{33}$$

with $p_{\cap} = 2$ and $p_{\sqcap^2} = 2$ so that $p_{\cap * \sqcap^2} = 4$. This kernel is plotted in Fig. 11.

– *Smoothness* $m_{\cap} \in C^{\infty}_c(\mathbb{R}^n)$, so that $\langle g \rangle^f_{\cap * \wedge} \in C^{\infty}(\mathbb{R}^n)$. Figure 12 shows this for the second-order derivatives and model porous structures.
– *Fluctuations* as shown in Fig. 12, $m_{\cap * \wedge}$ is very efficient at filtering the fluctuations induced by the geometry of the porous medium.
– *Effect on a periodic function* it also has the property that, if a is periodic, then

$$\langle a \rangle^f_{\cap * \wedge} = \langle a \rangle^f_{\sqcap}. \tag{34}$$

This gives it the same advantage as $m_{\wedge}$ for the calculation of effective parameters on a single unit cell.
– *Quasiperiodicity* $m_{\cap * \wedge}$ is efficient at filtering out the fluctuations in the linear case and as efficient as $m_{\sqcap^q}$ for the random displacement (Fig. 12).

3.4 Negative Kernels

Here, we consider negative kernels that are built using the sinc function,

$$m_{\sim}(\mathbf{x}) \equiv \prod_{i=1}^{n} \operatorname{sinc}(x_i), \tag{35}$$

with

$$\operatorname{sinc}(x) = \frac{\sin(\pi x)}{\pi x},$$

implicitly defined for sinc and all its derivatives at $x = 0$. $m_{\sim}$ is the ideal low-pass filter because the Fourier transform of the sinc is a rectangular function, therefore filtering perfectly in the frequency domain. Its properties are as follows:

– *Smoothness* $m_{\sim}$ is $C^{\infty}(\mathbb{R}^n)$ and $\langle g \rangle^f_{\sim} \in C^{\infty}(\mathbb{R}^n)$.
– *Fluctuations* $m_{\sim}$ filters all fluctuations induced by the porous medium geometry perfectly. For instance, we have (proof in Appendix 7.1)

$$\langle \mathcal{P}_i \rangle^f_{\sim} = \mathcal{P}_i. \tag{36}$$

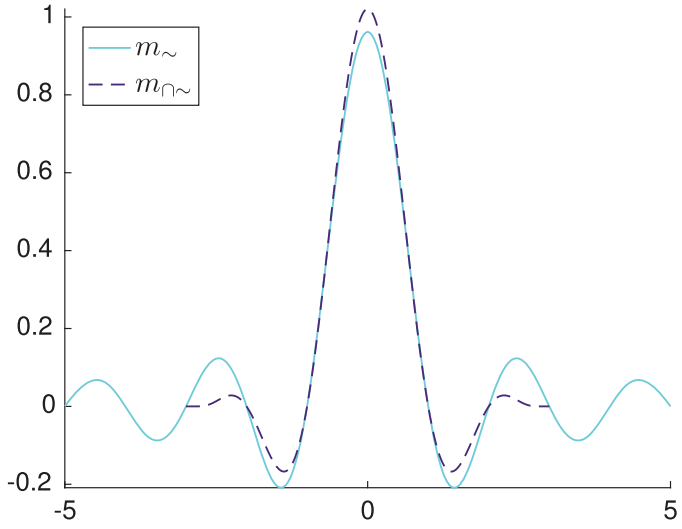

Fig. 13 One-dimensional sinc kernels used in the spatial convolution. $m_\sim$ and $m_{\cap\sim}$ are, respectively, the sinc and windowed sinc kernels

– *Effect on a periodic function* $m_\sim$ has the property that, if a is periodic, then (proof in Appendix 7.1)

$$\langle a \rangle_\sim^f = \langle a \rangle_\sqcap^f . \tag{37}$$

– *Taylor series* it is particulary useful for Taylor series approximations, as we detail in the next section.

Negative kernels do not necessarily respect the positivity of the fields, especially close to strong gradients (similar situations occur with shocks in smoothed particle hydrodynamics (Monaghan 2005)). An obvious example of this is the case where the initial condition of the field is a Dirac delta, so that the average field is the sinc function. For the VAT, however, this is not a major issue because we already have implicit constraints regarding the amplitude of the gradients, i.e., the characteristic lengthscale for variation of the fields is much larger than the size of the unit cell, thus eliminating the possibility of having a Dirac delta for instance. The main problem of $m_\sim$ is actually that it has infinite support in the time domain (it is compactly supported in the frequency domain). This considerably reduces its practical use. One way to circumvent this problem consists in windowing the sinc using the mollifier kernel (this could be done in a number of other ways), and we define

$$m_{\cap\sim} = m_\cap m_\sim . \tag{38}$$

Both kernels are plotted in Fig. 13. The properties of this new kernel can be summarized as

– *Smoothness* $m_{\cap\sim} \in C^\infty(\mathbb{R}^n)$, so that $\langle g \rangle_{\cap\sim}^f \in C^\infty(\mathbb{R}^n)$. Figure 14 shows this for the first-order derivatives and model porous structures.
– *Fluctuations* as shown in Fig. 14, the ability of $m_{\cap\sim}$ depends mostly on the support of the function, with the perturbations going to zero in the limit of infinite support when we recover the sinc function.
– *Effect on a periodic function* in general,

$$\langle g \rangle_{\cap\sim}^f \neq \langle g \rangle_\sqcap^f , \tag{39}$$

with $\langle g \rangle_{\cap\sim}^f = \langle g \rangle_\sqcap^f$ in the limit $p_{\cap\sim} \to \infty$.
– *Quasiperiodicity* we do not show the results here, but the $m_{\cap\sim}$ is as efficient as $m_{\sqcap^q}$ at filtering fluctuations in quasiperiodic configurations.

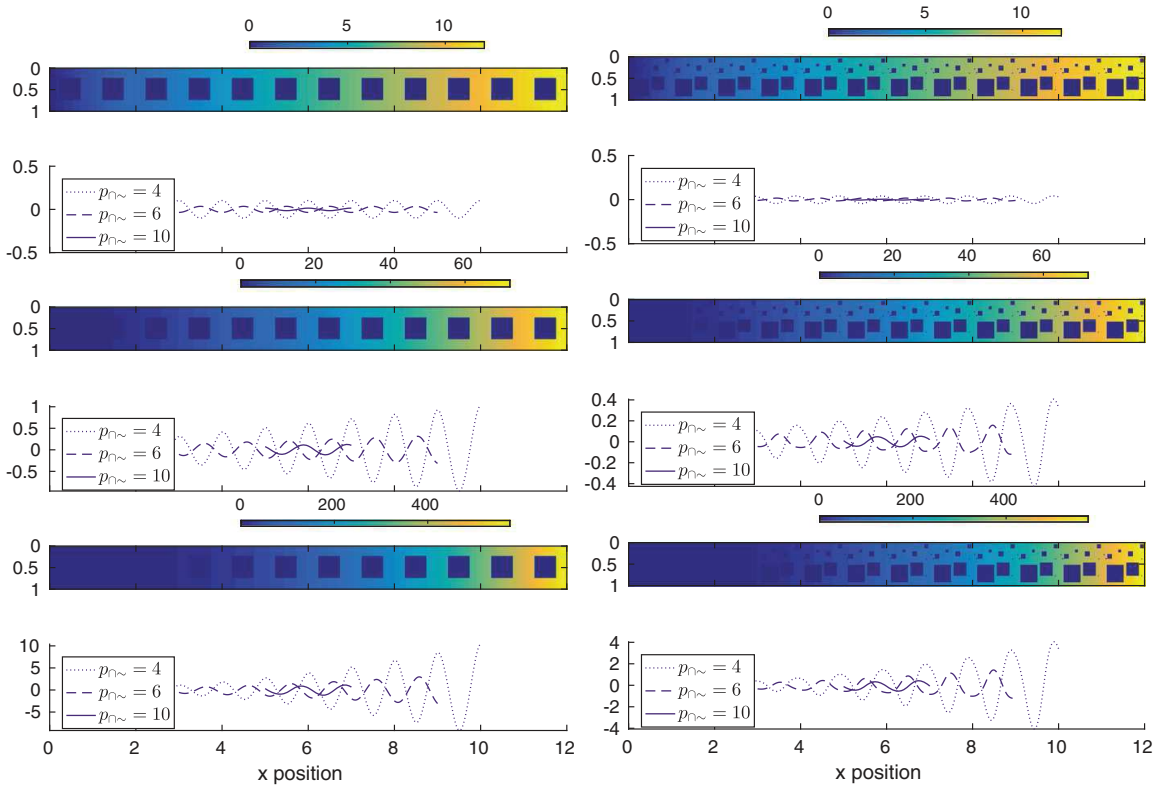

Fig. 14 First-order derivatives of the average of polynomial fields obtained for ordered (*left-hand side*) and slightly disordered (*right-hand side*) periodic structures. The first rows represent the field $\chi^f \mathcal{P}_1$, and the second rows are the derivatives $d_x \langle \mathcal{P}_1 \rangle^f_{\cap\sim} - d_x \mathcal{P}_1$. The following rows are similar, but for $\mathcal{P}_2$ and $\mathcal{P}_3$

4 Taylor Series in the VAT

In the VAT, we are often led to use Taylor series in order to express and localize successive averages of the same field. Here, we consider the quantity $\left\langle a\,(\mathbf{r})\ \langle g \rangle^f \big|_{\mathbf{r}} \right\rangle^f \Big|_{\mathbf{x}}$ with a periodic of period 1. a can therefore be expressed as the Fourier series,

$$a = a_0 + \sum_{k \neq 0} a_n e^{2i\pi kx}, \tag{40}$$

where a_0 is the constant part, which may also be expressed as $a_0 = \langle a \rangle^f_{\sqcap}$. If the kernel is such that $\langle g \rangle^f \in C^M(\mathbb{R}^n)$, then we can write

$$\left\langle a\,(\mathbf{r})\ \langle g \rangle^f \Big|_{\mathbf{r}} \right\rangle^f \Big|_{\mathbf{x}} = \sum_{j=0}^{M} (-1)^j \frac{1}{j!} \left. \frac{(m \wp_j) * (a \chi^f)}{m * \chi^f} \right|_{\mathbf{x}} (\cdot)^j\ \nabla^{\otimes j} \langle g \rangle^f \Big|_{\mathbf{x}} + \mathcal{O}\left(\varepsilon^{M+1}\right), \tag{41}$$

with $\varepsilon = \frac{\ell_u}{L}$, $\ell_u = 1$ the size of the unit cell, L a macroscopic lengthscale, $\boldsymbol{\xi}^{\otimes j}$ the tensorial product $\boldsymbol{\xi}^{\otimes j} = \underbrace{\boldsymbol{\xi} \otimes \cdots \otimes \boldsymbol{\xi}}_{\text{j times}}$, $\nabla^{\otimes j} = \underbrace{\nabla \otimes \cdots \otimes \nabla}_{\text{j times}}$, $(\cdot)^j$ the jth order tensorial contraction and $\wp_j(\mathbf{x}) = \mathbf{x}^{\otimes j}$ (derivation in Appendix 7.2). For instance, for $M = 2$, we have

$$\left\langle \langle g \rangle^f \Big|_{\mathbf{r}} \right\rangle^f \Big|_{\mathbf{x}} = \langle a \rangle^f \Big|_{\mathbf{x}} \langle g \rangle^f \Big|_{\mathbf{x}} - \left. \frac{(m\wp_1) * \left(a\chi^f\right)}{m * \chi^f} \right|_{\mathbf{x}} \cdot \nabla \langle g \rangle^f \Big|_{\mathbf{x}}, + \frac{1}{2} \left. \frac{(m\wp_2) * \left(a\chi^f\right)}{m * \chi^f} \right|_{\mathbf{x}} : \nabla\nabla \langle g \rangle^f \Big|_{\mathbf{x}} + \mathcal{O}\left(\varepsilon^3\right). \tag{42}$$

Ideally, we want to use a kernel that simplifies the Taylor series. To do so, we would like

$$\frac{\left(m\wp_j\right) * \left(a\chi^f\right)}{m * \chi^f} = 0. \tag{43}$$

Does such a kernel exist? Not if $m > 0$ and $a_0 \neq 0$. For example, consider $a = 1$ and the integral $\int_{\mathbb{R}^n} (m\wp_2) * \chi^f \mathrm{d}\mathbf{x}$. With $m\wp_2$ and χ^f positive, we have

$$\frac{(m\wp_2) * \chi^f}{m * \chi^f} > 0. \tag{44}$$

Can we build a positive kernel that almost satisfies this condition? Yes, $m = m_{\sqcap^q}$ does. Indeed, we can show that (demonstration for $n = 1$ in "Appendix" 7.3)

$$\frac{\left(m_{\sqcap^q}\wp_j\right) * \left(a\chi^f\right)}{m_{\sqcap^q} * \chi^f} = a_0 \mathcal{M}_{j,q}, \tag{45}$$

with $\mathcal{M}_{j,q}$ the jth moment of $m_{\sqcap^q}$ expressed as

$$\mathcal{M}_{j,q} = \int_{\mathbb{R}^n} m_{\sqcap^q}(\mathbf{x})\, \wp_j(\mathbf{x})\, d\mathbf{x}. \tag{46}$$

The demonstration (for $n = 1$ in Appendix 7.3) uses Fourier transforms to show that the only overlap between frequencies of $m_{\sqcap^q}\wp_j$ and $a\chi^f$ is in 0, so that only the constant part of the periodic function remains.

With the symmetries of $m_{\sqcap^q}(\mathbf{x})$, we have that $\mathcal{M}_{j,q} = 0$ if j is odd. Therefore, we can summarize this as

$$a_0 = \langle a \rangle_{\sqcap}^f = 0 \Rightarrow \frac{\left(m_{\sqcap^q}\wp_j\right) * \left(a\chi^f\right)}{m_{\sqcap^q} * \chi^f} = 0. \tag{47}$$

Otherwise,

$$\left\langle \frac{a}{a_0}(\mathbf{r})\, \langle g \rangle^f \Big|_{\mathbf{r}} \right\rangle^f \Big|_{\mathbf{x}} = \sum_{j=0}^{M} (-1)^j \frac{1}{j!} \mathcal{M}_{j,q}\, (\cdot)^j\, \nabla^{\otimes j} \langle g \rangle^f \Big|_{\mathbf{x}} + \mathcal{O}\left(\varepsilon^{M+1}\right), \tag{48}$$

with $\mathcal{M}_{j,q} = 0$ if j is odd. The case $a_0 = 0$ is actually important, because for most closure variables in the VAT this property is verified.

Can we obtain a negative kernel that satisfies $\left(m\wp_j\right) * \left(a\chi^f\right) = 0$ exactly? Yes, $m_{\sim}$ does (demonstration for $n = 1$ in Appendix), and this is a very important property of the sinc function. It is the perfect low-pass filter, filtering all lengthscales smaller or equal to the size of the unit cell. Therefore, the sinc is, in theory, the ideal filter for the VAT with regard to frequency filtering, but in practice we must use a windowed version of it such as $m_{\cap\sim}$, so that its advantage becomes unclear compared to positive kernels.

5 VAT for Stokes' Flow

In this section, we apply the VAT to the problem of Stokes flow in a porous medium to show how to derive Darcy's law, a problem that was also discussed in Whitaker (1986), Quintard and Whitaker (1994), Buckinx and Baelmans (2015b). In doing so, our goal is to provide a simple example of derivation and show precisely what properties of the kernel are important and when they are used in the VAT. To do so, we first consider a generic kernel that we do not specify and construct it step by step. Stokes' equation reads

$$-\nabla P(\mathbf{x}) + \nabla \cdot \left[\mu\left(\nabla \mathbf{v} +^{\mathsf{T}} (\nabla \mathbf{v})\right)\right](\mathbf{x}) = -\rho \mathbf{g}. \tag{49}$$

The average equation is

$$\left\langle -\nabla P + \nabla \cdot \left[\mu\left(\nabla \mathbf{v} +^{\mathsf{T}} (\nabla \mathbf{v})\right)\right]\right\rangle^f \Big|_{\mathbf{x}} = -\rho \mathbf{g}, \tag{50}$$

with ρ and μ constant. Subtracting Eq. 50 from Eq. 49, we obtain

$$-\nabla P(\mathbf{x}) + \nabla \cdot \left[\mu\left(\nabla \mathbf{v} +^{\mathsf{T}} (\nabla \mathbf{v})\right)\right](\mathbf{x}) = \left\langle -\nabla P + \nabla \cdot \left[\mu\left(\nabla \mathbf{v} +^{\mathsf{T}} (\nabla \mathbf{v})\right)\right]\right\rangle^f \Big|_{\mathbf{x}}. \tag{51}$$

We also have

$$\mathbf{v}(\mathbf{x}) = 0, \tag{52}$$

on the solid interface. As usual Whitaker (1986, 1999), we look for a solution to this problem in the form

$$P(\mathbf{x}) = \langle P \rangle^f \Big|_{\mathbf{x}} + \mu \mathbf{b}(\mathbf{x}) \cdot \langle \mathbf{v} \rangle^f \Big|_{\mathbf{x}}, \tag{53}$$

for the pressure and

$$\mathbf{v}(\mathbf{x}) = \mathbf{B}(\mathbf{x}) \cdot \langle \mathbf{v} \rangle^f \Big|_{\mathbf{x}}, \tag{54}$$

for the velocity, with $\mathbf{b}$ and $\mathbf{B}$ locally periodic.

To obtain the average conditions, we first average Eq. 53 in space to obtain

$$\langle P \rangle^f \Big|_{\mathbf{x}} = \left\langle \langle P \rangle^f \Big|_{\mathbf{r}} \right\rangle^f \Big|_{\mathbf{x}} + \mu \left\langle \mathbf{b}(\mathbf{r}) \cdot \langle \mathbf{v} \rangle^f \Big|_{\mathbf{r}} \right\rangle^f \Big|_{\mathbf{x}}. \tag{55}$$

We now require that the kernel is such that $\langle P \rangle^f \in C^1(\mathbb{R}^n)$, so that we can use a first-order Taylor expansion as

$$\left\langle \langle P \rangle^f \Big|_{\mathbf{r}} \right\rangle^f \Big|_{\mathbf{x}} = \langle P \rangle^f \Big|_{\mathbf{x}} + \langle \mathbf{x} - \mathbf{r} \rangle^f \Big|_{\mathbf{x}} \cdot \nabla \langle P \rangle^f \Big|_{\mathbf{x}} + \mathcal{O}\left(\varepsilon^2\right). \tag{56}$$

To simplify this, we now need $\langle \mathbf{x} - \mathbf{r} \rangle^f \big|_{\mathbf{x}} = 0$, which is satisfied exactly by $m_\wedge$ (or any $m_{\sqcap^{q>1}}$) and $m_\sim$, but only approximately by $m_{\cap\sim}$. Therefore, the simplest compactly supported kernel that is sufficient at this stage is $m_{\sqcap^2} = m_\wedge$. We can only do this because we have a first-order closure (i.e., second-order derivatives of the pressure and first-order derivatives of the velocity are neglected). In the remainder of this section, we therefore consider $m = m_\wedge$. With $\langle \mathbf{x} - \mathbf{r} \rangle^f_\wedge \Big|_{\mathbf{x}} = 0$ verified exactly, we have

$$\left\langle \langle P \rangle^f_\wedge \Big|_{\mathbf{r}} \right\rangle^f \Big|_{\mathbf{x}} = \langle P \rangle^f_\wedge \Big|_{\mathbf{x}} + \mathcal{O}\left(\varepsilon^2\right). \tag{57}$$

Similarly,

$$\left\langle \mathbf{b}\left(\mathbf{r}\right)\cdot\left\langle \mathbf{v}\right\rangle _{\wedge}^{f}\Big|_{\mathbf{r}}\right\rangle _{\wedge}^{f}\Big|_{\mathbf{x}}=\left\langle \mathbf{b}\right\rangle _{\wedge}^{f}\Big|_{\mathbf{x}}\cdot\left\langle \mathbf{v}\right\rangle _{\wedge}^{f}\Big|_{\mathbf{x}}+\left\langle \mathbf{b}\otimes\left(\mathbf{x}-\mathbf{r}\right)\right\rangle _{\wedge}^{f}\Big|_{\mathbf{x}}\cdot\nabla\left\langle \mathbf{v}\right\rangle _{\wedge}^{f}\Big|_{\mathbf{x}}+\mathcal{O}\left(\varepsilon^{2}\right). \tag{58}$$

We have seen that $\left\langle \mathbf{b}\left(\mathbf{r}\right)\otimes\left(\mathbf{x}-\mathbf{r}\right)\right\rangle _{\wedge}^{f}=0$ so that

$$\left\langle \mathbf{b}\left(\mathbf{r}\right)\cdot\left\langle \mathbf{v}\right\rangle _{\wedge}^{f}\Big|_{\mathbf{r}}\right\rangle _{\wedge}^{f}\Big|_{\mathbf{x}}=\left\langle \mathbf{b}\right\rangle _{\wedge}^{f}\Big|_{\mathbf{x}}\cdot\left\langle \mathbf{v}\right\rangle _{\wedge}^{f}\Big|_{\mathbf{x}}+\mathcal{O}\left(\varepsilon^{2}\right), \tag{59}$$

and Eq. 58 reads

$$\left\langle \mathbf{b}\right\rangle _{\wedge}^{f}\Big|_{\mathbf{x}}\cdot\left\langle \mathbf{v}\right\rangle _{\wedge}^{f}\Big|_{\mathbf{x}}\simeq0. \tag{60}$$

This result must hold for any value of $\left\langle \mathbf{v}\right\rangle _{\wedge}^{f}\Big|_{\mathbf{x}}$, so that we impose

$$\left\langle \mathbf{b}\right\rangle _{\wedge}^{f}\Big|_{\mathbf{x}}=0. \tag{61}$$

For the velocity, the average condition reads

$$\left\langle \mathbf{v}\right\rangle _{\wedge}^{f}\Big|_{\mathbf{x}}=\left\langle \mathbf{B}\left(\mathbf{r}\right)\cdot\left\langle \mathbf{v}\right\rangle _{\wedge}^{f}\Big|_{\mathbf{r}}\right\rangle _{\wedge}^{f}\Big|_{\mathbf{x}}, \tag{62}$$

and with similar manipulations we find

$$\left\langle \mathbf{v}\right\rangle _{\wedge}^{f}\Big|_{\mathbf{x}}=\left\langle \mathbf{B}\right\rangle _{\wedge}^{f}\Big|_{\mathbf{x}}\cdot\left\langle \mathbf{v}\right\rangle _{\wedge}^{f}\Big|_{\mathbf{x}}+\mathcal{O}\left(\varepsilon^{2}\right), \tag{63}$$

and impose

$$\left\langle \mathbf{B}\right\rangle _{\wedge}^{f}\Big|_{\mathbf{x}}=\mathbf{I}. \tag{64}$$

We have $\left\langle g\right\rangle _{\wedge}^{f}=\left\langle g\right\rangle _{\sqcap}^{f}$ for g periodic, so that

$$\left\langle \mathbf{b}\right\rangle _{\sqcap}^{f}\Big|_{\mathbf{x}}=0. \tag{65}$$

$$\left\langle \mathbf{B}\right\rangle _{\sqcap}^{f}\Big|_{\mathbf{x}}=\mathbf{I}. \tag{66}$$

The closure problems at the center of the unit cell, $\mathbf{X}$, therefore reads

$$-\nabla\mathbf{b}+\nabla\cdot\left(\nabla\mathbf{B}+^{\mathsf{T}}\left(\nabla\mathbf{B}\right)\right) = \left\langle -\nabla\mathbf{b}+\nabla\cdot\left(\nabla\mathbf{B}+^{\mathsf{T}}\left(\nabla\mathbf{B}\right)\right)\right\rangle _{\sqcap}^{f}\Big|_{\mathbf{X}} \tag{67}$$

$$\left\langle \mathbf{B}\right\rangle _{\sqcap}^{f}\Big|_{\mathbf{X}} = \mathbf{I} \tag{68}$$

$$\left\langle \mathbf{b}\right\rangle _{\sqcap}^{f}\Big|_{\mathbf{X}} = 0 \tag{69}$$

$$\text{Periodicity.} \tag{70}$$

Finally, recall that the macroscale equation reads

$$\left\langle -\nabla P+\nabla\cdot\left[\mu\left(\nabla\mathbf{v}+^{\mathsf{T}}\left(\nabla\mathbf{v}\right)\right)\right]\right\rangle _{\wedge}^{f}\Big|_{\mathbf{x}}=-\rho\mathbf{g}. \tag{71}$$

Using the previous expressions, we can obtain

$$\left\langle \mathbf{v}\right\rangle _{\wedge}|_{\mathbf{x}}=-\frac{\mathbf{K}}{\mu}\cdot\left(\nabla\left\langle P\right\rangle _{\wedge}^{f}\Big|_{\mathbf{x}}-\rho\mathbf{g}\right)+\mathcal{O}\left(\varepsilon^{2}\right), \tag{72}$$

with

$$\mathbf{K} = \phi \left(\left\langle \nabla \mathbf{b} - \nabla \cdot \left(\nabla \mathbf{B} +^{\mathsf{T}} (\nabla \mathbf{B}) \right) \right\rangle_{\sqcap}^{f} \right)^{-1}. \tag{73}$$

This is often expressed as a surface average (see Whitaker (1999))

$$\mathbf{K} = \phi \left(\frac{1}{|\mathcal{Y}^f|} \int_{\partial \mathcal{Y}^{fs}} \mathbf{n}^{fs} \cdot \left[\mathbf{I}\mathbf{b} - \left(\nabla \mathbf{B} +^{\mathsf{T}} (\nabla \mathbf{B}) \right) \right] d\Sigma \right)^{-1}, \tag{74}$$

with $\mathcal{Y}$ the unit cell, $\partial \mathcal{Y}^{fs}$ the fluid–solid interface and $\mathbf{n}^{fs}$ the unit normal vector pointing from the fluid to the solid.

6 Summary and Conclusions

6.1 Summary of Properties of the Averaging Kernels for VAT

For VAT in a locally periodic porous medium, with the unit cell $\mathcal{Y}$ defined as the n-dimensional unit cube $[0, 1]^n$, the ideal kernel for frequency filtering and Taylor series approximations is the sinc function, $m_{\sim}$. An important property of $m_{\sim}$, which greatly simplifies Taylor series approximations, is that $\left(m_{\sim} \wp_j\right) * \left(g \chi^f\right) = 0$ with $\wp_j(\mathbf{x}) = \mathbf{x}^{\otimes j}$ for any $j \in \mathbb{N}^{+*}$. Although fundamentally important, this kernel is impractical because it is not compactly supported.

We therefore define a set of acceptable compactly supported kernels for practical use in the VAT as

$$\begin{aligned}
\{m \mid\ & (1)\ m \text{ generates a low-pass filter,} \\
& (2)\ m \text{ is normalized so that } \int m = 1, \\
& (3)\ m \text{ is compactly supported on } [-p/2, p/2]^n, \\
& (4)\ m \text{ is symmetric regarding each variable } x_i, \\
& (5)\ m * g \in C^k\left(\mathbb{R}^n\right) \text{ where } k \text{ is the order of the closure,} \\
& (6)\ m * a = m_{\sqcap} * a \text{ for } a \text{ periodic,} \\
& (7)\ \frac{\left(m \wp_j\right) * \left(a \chi^f\right)}{m * \chi^f} = \begin{cases} 0 & \text{if } j \leq k \text{ is odd} \\ \text{constant} & \text{if } j \leq k \text{ is even} \end{cases} \text{ for } a \text{ periodic. } \}
\end{aligned}$$

All the corresponding properties for the kernels used in this study are summarized in Table 1. We see that the property 7 eliminates the kernel $m_{\sqcap\sim}$, which does not yield $\left(m \wp_j\right) * \left(a \chi^f\right) = 0$ for j odd and that the only kernel that is suited is $m_{\sqcap^k}$ with k the order of the closure.

As we have seen for the case of Stokes' flow, there is an important correspondence between the order of the closure in the VAT and the definition of the kernel. First, we only need properties (4) and (7) up to the order of the closure k (largest order of the derivatives in the approximate form of the perturbation). Second, the case of the first-order closure, $k = 1$, is special because $(m \wp_1) * \left(a \chi^f\right) = 0$ can be obtained with $m_{\wedge}$ or any $m_{\sqcap^{q \geq 2}}$. Therefore, if the VAT is limited to first-order closure, we can use $m_{\sqcap^{q \geq 2}}$ and have all the necessary properties for the average fields. As soon as $k > 1$, we cannot readily obtain $\left(m \wp_j\right) * \left(a \chi^f\right) = 0$ with j even and a compactly supported function.

Table 1 Summary of the properties of the kernels

	$m_{\sqcap}$	$m_{\sqcap^{q>k}}$	$m_{\cap}$	$m_{\cap *\wedge}$	$m_{\sim}$	$m_{\cap\sim}$
Compact support?	Yes	Yes	Yes	Yes	No	Yes
Symmetric?	Yes	Yes	Yes	Yes	Yes	Yes
Smoothness of $m * g$?	C^0	C^q	C^∞	C^∞	C^∞	C^∞
$m * g = m_{\sqcap} * g$?	Yes	Yes	No	Yes	Yes	No
$\frac{(m_{\sqcap^q} \wp_j) * \left(g \chi^f\right)}{m_{\sqcap^q} * \chi^f} = \begin{cases} 0 & \text{if } j \text{ is odd} \\ c & \text{if } j \text{ is even} \end{cases}$?	No	Yes ($q > j$)	No	No	Yes ($c = 0$)	No
Reduces fluctuations compared to $m_{\sqcap}$?	—	Yes	Yes	Yes	Yes	Yes
Resilient to quasiperiodicity?	No	Yes	Yes	Yes	Yes	Yes

6.2 Conclusions

In this paper, we revisit the use of spatial convolution to perform spatial averaging with mathematical properties that are adapted to the VAT. In particular, we provide an improved and detailed analysis of the choice of the kernel for periodic and quasiperiodic media. Critical considerations turn out to be: the smoothness of the average field, the localization of the closure field for the calculation of effective parameters over a single unit cell, the ability to filter out the frequencies of the periodic microstructure, simplifications of Taylor series developments and the response of the average to perturbations from the strict periodicity.

Other important points to remember are as follows:

- How do we perform upscaling for locally periodic porous media? We have shown that upscaling can be performed using a generalized version of the averaging based on a spatial convolution with adequate kernels. In some cases, the fields can be regularized *a posteriori* , but this should be avoided primarily because it breaks some of the properties of average fields needed in the VAT.
- What is the best kernel for a periodic geometry? If the VAT is limited to first-order closure, use $m_{\sqcap^{q\geq 2}}$. Otherwise, we have shown that $m = m_{\sqcap^{q>k}}$ with k the order of the closure is perfectly suited to the VAT for periodic and quasiperiodic media. This point has been somehow overlooked in the previous works suggesting the use of multiple averaging.
- What is the best kernel for a quasiperiodic geometry? The performance of most kernels tested is similar regarding quasiperiodicity. The criteria for the choice of the kernel in a quasiperiodic configuration are (1) the desired smoothness of the average fields and (2) the width of the averaging kernel, which may be important to capture a random perturbation from the strict periodic situation.
- Does increasing the width of the averaging kernel help regularizing the average fields? It depends on the kernels and the geometry. In general, larger width are useful to reduce fluctuations in quasiperiodic configurations. For periodic geometries, especially for $m_{\sqcap}$, it does not regularize the fields, contrary to what was suggested in Howes and Whitaker (1985).
- Does it mean that studies in the literature using only $m_{\sqcap}$ are obsolete? The results presented here are important fundamentally to better understand the VAT and the link between the microscale and average fields. However, they have limited practical impact on the results in the literature. In most cases, the macroscale models derived in previous works generally assume the correct smoothness and neglect terms involving $\mathbf{x} - \mathbf{r}$ in

the Taylor series and closure problems. Therefore, the only point that is affected is the interpretation of the average fields, besides, of course, a more accurate mathematical framework. In fact, we even recommend to proceed in this way: perform the upscaling assuming an ideal averaging operator and then determine the kernel that is best suited to the practical case of interest.

7 Appendix

7.1 Properties of the sinc in One Dimension ($n = 1$)

First, we show that

$$\left\langle \mathcal{P}_j \right\rangle_{\sim}^{f} = \mathcal{P}_j, \tag{75}$$

with

$$\mathcal{P}_j : \; x \to \frac{1}{j} x^j, \tag{76}$$

in one dimension for simplicity. We start from the definition of the average,

$$\left\langle \mathcal{P}_j \right\rangle_{\sim}^{f} = \frac{m_{\sim} * \left(\chi^f \mathcal{P}_j \right)}{m_{\sim} * \chi^f}, \tag{77}$$

and define the Fourier transform of g as

$$\mathcal{F}(g)(w) = \int_{\mathbb{R}} g(x) \, e^{-2\pi i x w} \mathrm{d}x, \tag{78}$$

and the inverse Fourier transform $\mathcal{F}^{-1}$ as

$$\mathcal{F}^{-1}\left(\hat{g}\right)(x) = \int_{\mathbb{R}} \hat{g}(w) \, e^{+2\pi i w x} \mathrm{d}w. \tag{79}$$

For the Fourier transform of a convolution, we have the following property

$$\mathcal{F}\left[m_{\sim} * \left(\chi^f \mathcal{P}_j \right) \right] = \mathcal{F}(m_{\sim}) \, \mathcal{F}\left(\chi^f \mathcal{P}_j \right). \tag{80}$$

Here

$$\mathcal{F}(m_{\sim})(w) = R(w), \tag{81}$$

with R the rectangular function and

$$\mathcal{F}\left(\chi^f \mathcal{P}_j \right) = \frac{1}{j} \left(\frac{i}{2\pi} \right)^j \frac{\mathrm{d}^j \mathcal{F}\left(\chi^f \right)}{\mathrm{d}w^j}. \tag{82}$$

Further, χ^f is a periodic function so that it can be written as

$$\mathcal{F}\left(\chi^f \right)(w) = \sum_k \chi_k^f \, \delta(w - k), \tag{83}$$

and

$$\mathcal{F}\left(\chi^f \mathcal{P}_j \right)(w) = \frac{1}{j} \sum_k \chi_k^f \left(\frac{i}{2\pi} \right)^j \delta^{(j)}(w - k), \tag{84}$$

with $\delta^{(n)}$ the nth derivative of the Dirac. Therefore,

$$\mathcal{F}(m_\sim)\,\mathcal{F}\left(\chi^f \mathcal{P}_j\right)(w) = \frac{1}{j}\chi_0^f \left(\frac{i}{2\pi}\right)^j \delta^{(j)}(w), \tag{85}$$

$$= \chi_0^f \mathcal{F}\left(\mathcal{P}_j\right), \tag{86}$$

and, considering that $m_\sim * \chi^f = \chi_0^f$ and applying the inverse Fourier transform, we get

$$\frac{m_\sim * \left(\chi^f \mathcal{P}_j\right)}{m_\sim * \chi^f} = \mathcal{P}_j. \tag{87}$$

Next, we show that

$$\langle a\rangle_\sim^f = \langle a\rangle_\sqcap^f \tag{88}$$

for a periodic. With a similar analysis to that of before, we can easily obtain

$$\mathcal{F}(m_\sim)\,\mathcal{F}\left(\chi^f a\right)(w) = \chi_0^f a_0 \delta(w), \tag{89}$$

so that

$$\langle a\rangle_\sim^f = a_0 = \langle a\rangle_\sqcap^f \tag{90}$$

with a_0 the constant part in the Taylor series of a.

7.2 Taylor Series Developments

We first start with a Taylor series of $\langle g\rangle^f$, with g non-dimensionalized so that $\langle g\rangle^f = \mathcal{O}(1)$. Estimating the gradients of $\langle g\rangle^f$ as

$$\nabla^{\otimes j}\langle g\rangle^f\Big|_{\mathbf{x}} = \mathcal{O}\left(\frac{1}{L^j}\right), \tag{91}$$

with L a macroscopic lengthscale, we have

$$\langle g\rangle^f\Big|_{\mathbf{x}+(\mathbf{r}-\mathbf{x})} = \sum_{j=0}^{M} \frac{1}{j!}\wp_j(\mathbf{r}-\mathbf{x})\,(\cdot)^j\ \nabla^{\otimes j}\langle g\rangle^f\Big|_{\mathbf{x}} + \mathcal{O}\left(\varepsilon^{M+1}\right), \tag{92}$$

with $\varepsilon = \frac{\ell_u}{L}$ the ratio of the micro and macroscopic lengthscales and $\wp_j(\mathbf{r}-\mathbf{x}) = (\mathbf{r}-\mathbf{x})^{\otimes j}$. This allows us to express $\left\langle \langle g\rangle^f\big|_{\mathbf{r}}\right\rangle^f\Big|_{\mathbf{x}}$ as

$$\left\langle \langle g\rangle^f\Big|_{\mathbf{r}}\right\rangle^f\Big|_{\mathbf{x}} = \sum_{j=0}^{M} \frac{1}{j!}\left\langle \wp_j(\mathbf{r}-\mathbf{x})\right\rangle^f\Big|_{\mathbf{x}}(\cdot)^j\ \nabla^{\otimes j}\langle g\rangle^f\Big|_{\mathbf{x}} + \mathcal{O}\left(\varepsilon^{M+1}\right). \tag{93}$$

The convolution formulation of the averaging operator yields

$$\left\langle \wp_j(\mathbf{r}-\mathbf{x})\right\rangle^f\Big|_{\mathbf{x}} = \frac{1}{m * \chi^f}\int_{\mathbb{R}^n} m(\mathbf{x}-\mathbf{r})\,\wp_j(\mathbf{r}-\mathbf{x})\,\chi^f(\mathbf{r})\,\mathrm{d}\mathbf{r} \tag{94}$$

$$= (-1)^j\ \frac{\left(m\wp_j\right) * \left(a\chi^f\right)}{m * \chi^f}\Bigg|_{\mathbf{x}}. \tag{95}$$

Finally, we obtain

$$\left\langle \langle g\rangle^f\Big|_{\mathbf{r}}\right\rangle^f\Big|_{\mathbf{x}} = \sum_{j=0}^{M}(-1)^j\ \frac{1}{j!}\ \frac{\left(m\wp_j\right) * \left(a\chi^f\right)}{m * \chi^f}\Bigg|_{\mathbf{x}}(\cdot)^j\ \nabla^{\otimes j}\langle g\rangle^f\Big|_{\mathbf{x}} + \mathcal{O}\left(\varepsilon^{M+1}\right). \tag{96}$$

7.3 Demonstration of Eq. 45

We limit the demonstration to the one-dimensional case. The n-dimensional is similar, using the fact that functions are separable, but is very tedious and requires unusual definitions, such as the Fourier transform of Euclidean tensors. We consider the quantity

$$\frac{\left(m_{\sqcap^q} \wp_j\right) * \left(a\chi^f\right)}{m_{\sqcap^q} * \chi^f} = \frac{\left(m_{\sqcap^q} \wp_j\right) * \left(a\chi^f\right)}{m_{\sqcap} * \chi^f}. \tag{97}$$

The function $a\chi^f$ is periodic and can be written as

$$a\chi^f = a_0\chi_0^f + \sum_{k\neq 0} H_k e^{2i\pi kx}. \tag{98}$$

We use the Fourier transform, defined for a function $g : \mathbb{R} \to \mathbb{R}$ as

$$\mathcal{F}(g)(w) = \int_{\mathbb{R}} g(x)\, e^{-2\pi i x w} \mathrm{d}x, \tag{99}$$

and the inverse Fourier transform $\mathcal{F}^{-1}$ as

$$\mathcal{F}^{-1}\left(\hat{g}\right)(x) = \int_{\mathbb{R}} \hat{g}(w)\, e^{+2\pi i w x} \mathrm{d}w. \tag{100}$$

For the rectangular function, $m_{\sqcap}$, we therefore have

$$\mathcal{F}(m_{\sqcap})(w) = \mathrm{sinc}(w). \tag{101}$$

In addition, the Fourier transform of a convolution can be written as

$$\mathcal{F}(f * g) = \mathcal{F}(f)\,\mathcal{F}(g). \tag{102}$$

so that

$$\mathcal{F}(m_{\sqcap^q})(w) = \mathrm{sinc}^q(w), \tag{103}$$

and

$$\mathcal{F}\left[\left(m_{\sqcap^q} \wp_j\right) * \left(a\chi^f\right)\right] = \mathcal{F}\left(m_{\sqcap^q} \wp_j\right)\mathcal{F}\left(a\chi^f\right). \tag{104}$$

First, we have

$$\mathcal{F}\left(m_{\sqcap^q} \wp_j\right)(w) = \left(\frac{i}{2\pi}\right)^j \frac{d^j\left[\mathrm{sinc}^q\right]}{dw^j}(w) \tag{105}$$

Second,

$$\mathcal{F}\left(a\chi^f\right)(w) = a_0\chi_0^f\,\delta(w) + \sum_{k\neq 0} H_k\,\delta(w-k). \tag{106}$$

Therefore,

$$\begin{aligned}\mathcal{F}\left[\left(m_{\sqcap^q} \wp_j\right) * \left(a\chi^f\right)\right] = \left(\frac{i}{2\pi}\right)^j \frac{d^j\left[\mathrm{sinc}^q\right]}{dw^j}(w)\, a_0\chi_0^f\,\delta(w). \\ + \sum_{k\neq 0} H_k \left(\frac{i}{2\pi}\right)^j \frac{d^j\left[\mathrm{sinc}^q\right]}{dw^j}(w)\,\delta(w-k).\end{aligned} \tag{107}$$

For $k \in \mathbb{N}^{+*}$, we have

$$\frac{d^j\left[\mathrm{sinc}^q\right]}{dw^j}(w)\,\delta(w-k) = 0, \tag{108}$$

this being easily proved using the Faà di Bruno formula, which gives the jth derivative of a composition of functions. This yields

$$\mathcal{F}\left[\left(m_{\sqcap^q} \wp_j\right) * \left(a\chi^f\right)\right] = \left(\frac{i}{2\pi}\right)^j \frac{d^j\left[\mathrm{sinc}^q\right]}{dw^j}(w)\, a_0 \chi_0^f \delta(w), \tag{109}$$

$$= a_0 \chi_0^f \mathcal{F}\left(\mathcal{M}_{j,q}\right), \tag{110}$$

with

$$\mathcal{M}_{j,q} = \int_{\mathbb{R}} m_{\sqcap^q}(x)\, \wp_j(x)\, \mathrm{d}x. \tag{111}$$

Finally, applying the inverse Fourier transform, we obtain

$$\frac{\left(m_{\sqcap^q} \wp_j\right) * \left(a\chi^f\right)}{m_{\sqcap^q} * \chi^f} = a_0 \mathcal{M}_{j,q}, \tag{112}$$

the jth moment of $m_{\sqcap^q}$. In $\mathbb{R}^n$, this simply reads

$$\frac{\left(m_{\sqcap^q} \wp_j\right) * \left(a\chi^f\right)}{m_{\sqcap^q} * \chi^f} = a_0 \mathcal{M}_{j,q}, \tag{113}$$

with

$$\mathcal{M}_{j,q} = \int_{\mathbb{R}^n} m_{\sqcap^q}(\mathbf{x})\, \wp_j(\mathbf{x})\, \mathrm{d}\mathbf{x}. \tag{114}$$

References

Allain, H., Quintard, M., Prat, M., Baudouy, B.: Upscaling of superfluid helium flow in porous media. Int. J. Heat Mass Transf. **53**(21–22), 4852 (2010)

Baveye, P., Sposito, G.: The operational significance of the continuum hypothesis in the theory of water movement through soils and aquifers. Water Resour. Res. **20**(5), 521 (1984)

Buades, A., Coll, B., Morel, J.M.: A review of image denoising algorithms, with a new one. Multiscale Model. Simul. **4**(2), 490 (2005)

Buckinx, G., Baelmans, M.: Macro-scale heat transfer in periodically developed flow through isothermal solids. J. Fluid Mech. **780**, 274 (2015)

Buckinx, G., Baelmans, M.: Multi-scale modelling of flow in periodic solid structures through spatial averaging. J. Comput. Phys. **291**(C), 34 (2015)

Buckinx, G., Baelmans, M.: Macro-scale conjugate heat transfer in periodically developed flow through solid structures. J. Fluid Mech. **804**, 298 (2016)

Davit, Y., Byrne, H., Osborne, J., Pitt-Francis, J., Gavaghan, D., Quintard, M.: Hydrodynamic dispersion within porous biofilms. Phys. Rev. E **87**(1), 012718 (2013)

d'Hueppe, A., Chandesris, M., Jamet, D., Goyeau, B.: Boundary conditions at a fluid–porous interface for a convective heat transfer problem: analysis of the jump relations. Int. J. Heat Mass Transf. **54**(15), 3683 (2011)

Goyeau, B., Benihaddadene, T., Gobin, D., Quintard, M.: Numerical calculation of the permeability in a dendritic mushy zone. Metall. Mater. Trans. B **30**, 613 (1999)

Gray, W., Leijnse, A., Kolar, R., Blain, C.: Mathematical Tools for Changing Spatial Scales in the Analysis of Physical Systems. CRC Press, Boca Raton (1993)

Hassanizadeh, M., Gray, W.: General conservation equations for multi-phase systems: 1. Averaging procedure. Adv. Water Resour. **2**, 131 (1979)

Howes, F., Whitaker, S.: The spatial averaging theorem revisited. Chem. Eng. Sci. **40**, 1387 (1985)

Marle, C.: Application de la méthode de la thermodynamique des processus irréversibles à l'écoulement d'un fluide à travers un milieu poreux. Bull. RILEM **29**, 1066 (1965)

Marle, C.: Ecoulements monophasiques en milieu poreux. Rev. Inst. Fr. Pét. **22**, 1471 (1967)

Marle, C.: On macroscopic equations governing multiphase flow with diffusion and chemical reactions in porous media. Int. J. Eng. Sci. **20**(5), 643 (1982)

Mls, J.: On the existence of the derivative of the volume average. Transp. Porous Media **2**(6), 615 (1987)

Monaghan, J.: Smoothed particle hydrodynamics. Rep. Prog. Phys. **68**, 1703 (2005)
Ochoa-Tapia, J., Whitaker, S.: Momentum transfer at the boundary between a porous medium and a homogeneous fluid—I. Theoretical development. Int. J. Heat Mass Transf. **38**(14), 2635 (1995)
Quintard, M., Whitaker, S.: Transport in ordered and disordered porous media: volume-averaged equations, closure problems, and comparison with experiment. Chem. Eng. Sci. **48**(14), 2537 (1993)
Quintard, M., Whitaker, S.: Transport in ordered and disordered porous media I: the cellular average and the use of weighting functions. Transp. Porous Media **14**(2), 163 (1994)
Quintard, M., Whitaker, S.: Transport in ordered and disordered porous media II: generalized volume averaging. Transp. Porous Media **14**(2), 179 (1994)
Quintard, M., Whitaker, S.: Transport in ordered and disordered porous media IV: computer generated porous media for three-dimensional systems. Transp. Porous Media **15**(1), 51 (1994)
Quintard, M., Whitaker, S.: Transport in ordered and disordered porous media V: geometrical results for two-dimensional systems. Transp. Porous Media **15**, 183 (1994)
Quintard, M., Whitaker, S.: Transport in ordered and disordered porous media III: closure and comparison between theory and experiment. Transp. Porous Media **15**, 31 (1994)
Sagaut, P.: Large Eddy Simulation for Incompressible Flows. Scientific Computation. Springer, Berlin (2006)
Schwartz, L.: Théorie des distributions. Hermann, Paris (1978)
Strichartz, R.: A Guide to Distribution Theory and Fourier Transforms. CRC Press, Boca Raton (1994)
Valdés-Parada, F., Goyeau, B., Ochoa-Tapia, J.: Jump momentum boundary condition at a fluid-porous dividing surface: derivation of the closure problem. Chem. Eng. Sci. **62**, 4025 (2007)
Veverka, V.: Theorem for the local volume average of a gradient revised. Chem. Eng. Sci. **36**(5), 833 (1981)
Whitaker, S.: Flow in porous media I: a theoretical derivation of Darcy's law. Transp. Porous Media **1**(1), 3 (1986)
Whitaker, S.: The Method of Volume Averaging, Theory and Applications of Transport in Porous Media, vol. 13. Springer, Dordrecht (1999)
Witkin, A.P.: Scale-space filtering: a new approach to multi-scale description. In: IEEE International Conference on Acoustics, Speech, and Signal Processing, pp. 150–153 (1984)
Wood, B., Whitaker, S.: Diffusion and reaction in biofilms. Chem. Eng. Sci. **53**(3), 397 (1998)